COMPREHENSIVE ANALYSIS OF PHYSICAL LAYER PERFORMANCE FOR DSRC IN NLOS V2V SCENARIOS

by

SHUTING GUO

A dissertation submitted in partial fulfillment of the
requirements for the degree of

DOCTOR OF PHILOSOPHY
IN ELECTRICAL AND COMPUTER ENGINEERING

2024

Oakland University
Rochester, Michigan

Doctoral Advisory Committee:

Daniel N. Aloi, Ph.D., Chair
Jia Li, Ph.D.
Gary Barber, Ph.D.
Tamas Horvath, Ph.D.
Hongmei Zhao, Ph.D.

To my family for their love and encouragement

ACKNOWLEDGMENTS

I would like to present my deepest gratitude to my advisor, Professor Daniel N. Aloi, who has always provided me with the professional guidance on my Ph.D. study. I would also like to appreciate my committee members, Professor Jia Li, Professor Gary Barber, Professor Tamas Horvath, and Professor Hongmei Zhao, for their invaluable guidance and encouragement on my academic research. I am also grateful to the professors, faculties, and staffs of Oakland University for their generous help and support. I would also like to thank the experts, scholars, and friends for their precious suggestions and help on my way to pursue my dream.

Shuting Guo

ABSTRACT

COMPREHENSIVE ANALYSIS OF PHYSICAL LAYER PERFORMANCE FOR DSRC IN NLOS V2V SCENARIOS

by

SHUTING GUO

Adviser: Daniel N. Aloi, Ph.D.

Motivated by the development of the vehicle-to-everything (V2X) communications, both the dedicated short-range communications (DSRC) and the cellular V2X (C-V2X) involved in the radio access technologies (RATs) are experiencing extensive evolution to support advanced vehicular applications and scenarios. Both the DSRC and the C-V2X support the vehicle-to-vehicle (V2V), vehicle-to-infrastructure (V2I), and vehicle-to-pedestrian (V2P) communications to directly transmit and receive data between the vehicles, infrastructures, and pedestrians. In addition, the C-V2X can support the vehicle-to-network (V2N) communications via the cellular networks. However, the C-V2X suffers from the challenge in transmitting data within the permissible latency with the higher cellular network traffic load. On the contrary, in the DSRC with short-range wireless technologies, vehicles can directly communicate with each other to exchange information and to largely extend their awareness range beyond autonomous on-board capabilities. On one hand, IEEE 802.11p is more robust and mature with the large-scale field trials performed worldwide and can provide safety and service applications for the intelligent transportation system (ITS) in the vehicular

communications. On the other hand, IEEE 802.11bd was proposed as the amendment to IEEE 802.11p with the evolution for IEEE-based V2X communications by enhancing the reliability, throughput, and transmission range.

The contributions of the proposed work over the previous work are as follows. Firstly, extensive physical layer (PHY) metrics, containing the packet error rate (PER), packet reception ratio (PRR), output packet inter-arrival time (IAT), and output effective data rate, are sufficiently adopted to accomplish the thorough PHY evaluation which can avoid the limitation brought by the partial PHY metrics. Secondly, various multi-antenna configurations, including the multiple-input multiple-output (MIMO), single-input multiple-output (SIMO), and multiple-input single-output (MISO) systems, are added to remedy the incomplete analysis on antenna configurations induced by the only single-input single-output (SISO) configuration. Finally, considerably different packet sizes and modulation and coding schemes (MCSs) are discussed under the urban and highway non-line-of-sight (NLOS) scenarios to uncover the impact of each parameter on the PHY performance which cannot be found in the fixed parameter or slightly different parameters.

Some important conclusions obtained from a complete MATLAB-based PHY simulation are as follows. Firstly, the multi-antenna systems are more advantageous in reducing the PER, increasing the PRR and transmission coverage, decreasing the output packet IAT, and elevating the output effective data rate, compared to the SISO system, above the distance threshold and below the signal-to-noise ratio (SNR) threshold. Secondly, the packet size and the MCS should be adjusted simultaneously in different applications to accommodate their high-reliability, low-latency, or high-throughput requirement. Finally, the urban NLOS scenario with the lower Doppler effect is more tolerant than the highway NLOS scenario in the V2V communications due to its lower PER, larger PRR and transmission coverage, smaller output packet IAT, and higher output effective data rate.

TABLE OF CONTENTS

TABLE OF CONTENTS—Continued

LIST OF TABLES

LIST OF FIGURES

CHAPTER ONE

INTRODUCTION AND SCOPE OF WORK

The vehicle-to-everything (V2X) communications involved in the intelligent transportation system (ITS) have the potential and ability to not only improve the road safety, but also enhance the traffic management, energy efficiency, and air protection [1][2]. In 1999, the U.S. Federal Communications Commission (FCC) allocated the specific $75\ \text{MHz}$ licensed spectrum in the $5.9\ \text{GHz}$ frequency band ranging from $5.850\ \text{GHz}$ to $5.925\ \text{GHz}$ for the ITS to support both the vehicle-to-vehicle (V2V) and vehicle-to-infrastructure (V2I) communications by reducing the possible interference with other wireless devices [3][4][5]. Over the past two decades, this allocation has sparked major research activities around the world to develop and deploy the V2X communications aimed at addressing multiple challenges in its services, such as safety to vulnerable road users, smart navigation, cooperative maneuvering, and connected autonomous driving [6].

The radio access technologies (RATs), which can be divided into the dedicated short-range communications (DSRC) and the cellular V2X (C-V2X), are undergoing the extensive development and evolution for the more stringent vehicular scenarios and applications where the high-reliability, low-latency, or high-throughput requirement needs to be satisfied [1]. The DSRC operates within the $5.9\ \text{GHz}$ frequency band primarily, which has been designated for the ITS applications in the U.S., Europe, and many other countries [1][7]. The C-V2X can operate not only in the $5.9\ \text{GHz}$ frequency band but also in the licensed operating bands of the cellular operators [1][8].

As the basic standard for the vehicular ad hoc networks (VANETs), IEEE 802.11p was the first standardized DSRC technology for direct V2X communications [9]. Afterwards, the IEEE 802.11 group has been working towards IEEE 802.11bd [10][11], the next-generation V2X (NGV) standard, which is expected to greatly improve the performance compared to IEEE 802.11p with new physical layer (PHY) and medium access control (MAC) technologies [12][13][14]. On the other hand, as a substitute to IEEE 802.11p, the long-term evolution (LTE) was announced by the 3rd Generation Partnership Project (3GPP) in Release 14 with the advanced features based on the cellular technologies [15][16]. Moreover, the new radio V2X (NR-V2X) was issued as the next-generation C-V2X and fully specified in Release 16 which supports various use cases, multiple deployment options, and wide frequency bands with the flexible, scalable, and forward-compatible PHY and MAC layers [17][18].

In addition to the V2V, V2I, and vehicle-to-pedestrian (V2P) communications supported by both the DSRC and the C-V2X which can directly transmit and receive data between the vehicles, infrastructures, and pedestrians, the C-V2X can also support the vehicle-to-network (V2N) communications via cellular networks [19][20][21]. However, the C-V2X suffers from the challenge in transmitting data within the permissible latency with the higher cellular network traffic load [2][22][23]. With the short-range wireless technologies in the DSRC, the vehicles, infrastructures, and pedestrians can directly communicate with each other to exchange information and to largely extend their awareness range beyond autonomous on-board capabilities [24]. Designed as the key standard of the wireless access in vehicular environments (WAVE) architecture for the DSRC [25], IEEE 802.11p is more robust and mature with the large-scale field trials performed worldwide [8][22][26] and can provide safety and service applications for the ITS in the vehicular communications [3]. Meanwhile, IEEE 802.11bd was proposed as the amendment to IEEE 802.11p with the evolution for IEEE-based V2X communications by enhancing the reliability, throughput, and transmission range [26][27][28].

This Ph.D. dissertation research focuses on the evaluation on the PHY performance of both IEEE 802.11p and IEEE 802.11bd in terms of the packet error rate (PER), packet reception ratio (PRR), output packet inter-arrival time (IAT), and output effective data rate. The MATLAB-based simulation is implemented and analyzed with the single-input single-output (SISO), multiple-input single-output (MISO), single-input multiple-output (SIMO), and multiple-input multiple-output (MIMO) systems for distinct packet sizes and different modulation and coding schemes (MCSs) under both the urban non-line-of-sight (NLOS) and highway NLOS scenarios. Accordingly, the impact of the antenna configuration, packet size, MCS, and Doppler effect on the PHY performance are investigated and presented.

Consequently, this dissertation is organized as follows. The introduction and scope of our proposed work are given in chapter one. The related literatures on IEEE 802.11p and IEEE 802.11bd are reviewed in chapter two in comparison with the proposed work to present the contribution and significance of the dissertation research. The theories and technologies of the open systems interconnection (OSI) model, DSRC, line-of-sight (LOS) and NLOS propagation, V2V channel model, orthogonal frequency-division multiplexing (OFDM) and MIMO, and PHY metrics are provided in chapter three as the fundamentals to initiate our research. The simulation on IEEE 802.11p and IEEE 802.11bd are performed and analyzed in chapter four according to the PHY metrics including the PER, PRR, output packet IAT, and output effective data rate based on various antenna configurations, packet sizes, and MCSs in both the urban NLOS and highway NLOS scenarios. Finally, the dissertation is concluded in chapter five.

CHAPTER TWO

LITERATURE REVIEW

The following several literatures are dedicated to the performance estimation on the DSRC and the C-V2X standards.

It was pointed out in [29] that both the C-V2X technologies can support all the considered V2I services without any limitations based on the simulation which benchmarks their performance deployed for the V2I communications in an urban scenario. Additionally, the simulation and measurement with two antenna types located at three different heights were implemented in [30] with the C-V2X PC5 mode 4 interfaces under the rural scenario for the direct V2V communications. Moreover, the PHY performance comparison on both the C-V2X standards and both the DSRC standards was conducted in [31] according to the simulation on the V2V channel model under the urban NLOS scenario. Furthermore, it was indicated in [32] that, compared with the DSRC technology which can realize a smaller end-to-end delay and a higher packet delivery ratio (PDR) in the observed V2I communication scenarios, the LTE technology with the worse performance imposes additional limitations on the feasible applications. Besides, based on the system-level simulation fulfilled under the highway scenarios in [33], the DSRC performs better than the LTE with the smaller and stable data packet delay for the higher vehicle density. As the variant standard of the DSRC in Europe, the ITS-G5 was compared with the LTE-V2X PC5 under the real-life highway environment in [34] and provides the lower latency for the low-density V2I and V2V scenarios. In addition, based on the simulation fulfilled under the realistic urban scenarios in [35], the ITS-G5 outperforms the LTE-V2X PC 5 mode 3 on which the concurrent applications are scheduled. Moreover, the performance analysis on IEEE 802.11p and IEEE 802.11bd was proposed in [28] across multiple layers including the PHY for safety applications. Besides, the real-world performance of IEEE 802.11p was presented in [4] focusing on the maximum range and the PDR of the V2I communications.

Nevertheless, there are some gaps existing in the previous work on both IEEE 802.11p and IEEE 802.11bd which need to be bridged and thus our research is proposed to improve the PHY performance evaluation accordingly.

2.1 IEEE 802.11p

Confronted with the PER and PRR utilized in [36] with the only SISO channel under the highway LOS and NLOS scenarios for the fixed packet size and MCS, the latency and throughput metrics are neglected in the PHY evaluation and the influence of the multi-antenna configuration, Doppler effect, packet size, and MCS cannot be obtained. Since the PER and throughput considered in [26] are under the SISO channel model either for MCS 2 with the 100-byte packet or for MCS 5 with the 300-byte packet, the PRR and latency metrics are absent and the effect of the multi-antenna configuration, MCS, and packet size are not discussed. Although the PER, PRR, data rate, and packet IAT are adequately selected as the PHY metrics in [31] for the urban NLOS scenario with the SISO channel model, the highway NLOS scenario and the MIMO, SIMO, and MISO channel models are still indispensable to study the impact of the Doppler effect and multi-antenna configuration on the PHY performance.

To explicitly present and clarify the advantages and significance of the proposed work over the previous work, the detailed comparison of IEEE 802.11p between this work and the existing work on the adopted PHY metrics and the observed parameters is outlined in Table 2.1.

Table 2.1 Comparison on IEEE 802.11p between this work and existing work

Source	PHY Metric				Parameter			
	PER	PRR	Packet IAT	Data Rate	Antenna Configuration	Packet Size (bytes)	MCS	V2V Scenario
[36]	Yes	Yes	No	No	SISO	300	2	Highway LOS Highway NLOS
[26]	Yes	No	No	Yes	SISO	100 300	2 5	Rural LOS Urban LOS Highway LOS Urban NLOS Highway NLOS
[31]	Yes	Yes	Yes	Yes	SISO	100 1500	2/0 6	Urban NLOS
This Work	**Yes**	**Yes**	**Yes**	**Yes**	**SISO** **MISO** **SIMO** **MIMO**	**100** **1500**	**2** **6**	**Urban NLOS** **Highway NLOS**

2.2 IEEE 802.11bd

The parameters, performance, and mechanism of IEEE 802.11bd are introduced conceptually in [1] without any support of essential simulation results. On the contrary, the PHY simulation is conducted to provide the necessary support on the theoretical analysis in the following literatures. During the study on the reliability requirement in the SISO channel with the fixed packet size in [37], the PER is the unique metric employed which is not sufficient for the full PHY estimation and the impact of the multi-antenna configuration and packet size cannot be observed. Faced with the PER and PRR metrics under the SISO channel of the highway LOS and NLOS scenarios with the fixed packet size and MCS in [36], not only the PHY performance regarding the latency and throughput, but also the impact of the multi-antenna configuration, Doppler effect, packet size, and MCS cannot be realized in the investigation. Even though the complete PHY metrics, which involve the PER, PRR, data rate, and packet IAT, are chosen in [31] for the PHY evaluation on a SISO channel model under the urban NLOS scenario, the MIMO, SIMO, and MISO channel models and the highway NLOS scenario still should be added to explore the impact of the multi-antenna configuration and Doppler effect on the PHY performance. When the PER and throughput are analyzed in [26] either for the 1×1 antenna configuration with the 100-byte packet and MCS 1, or for the 2×1 and 2×2 antenna configurations with the 300-byte packet and MCS 4, the investigation on the PRR and latency metrics are still required and the effect of the antenna configuration, packet size, and MCS should not be ignored.

The detailed comparison of IEEE 802.11bd between this work and the existing work on the employed PHY metrics and investigated parameters is listed in Table 2.2 which can intuitively demonstrate the advantages and significance of the proposed work over the previous work.

Table 2.2 Comparison on IEEE 802.11bd between this work and existing work

Source	PHY Metric				Parameter			
	PER	PRR	Packet IAT	Data Rate	Antenna Configuration	Packet Size (bytes)	MCS	V2V Scenario
[1]	No	No	No	No	N/A	N/A	N/A	N/A
[37]	Yes	No	No	No	SISO	300	0 3	Rural LOS Urban LOS Urban NLOS Highway LOS Highway NLOS
[36]	Yes	Yes	No	No	SISO	300	1	Highway LOS Highway NLOS
[31]	Yes	Yes	Yes	Yes	SISO	100 1500	1/0 5	Urban NLOS
[26]	Yes	No	No	Yes	SISO	100	1	Rural LOS Urban LOS Highway LOS Urban NLOS Highway NLOS
					MISO MIMO	300	4	
This Work	**Yes**	**Yes**	**Yes**	**Yes**	**SISO** **MISO** **SIMO** **MIMO**	**100** **1500**	**1** **5**	**Urban NLOS** **Highway NLOS**

The main aspects of this proposed work contributed to IEEE 802.11p and IEEE 802.11bd are summarized as follows. Firstly, to avoid the limited PHY evaluation brought by the partial PHY metrics used in most previous literatures, the extensive PHY metrics, containing the PER, PRR, output packet IAT, and output effective data rate, are sufficiently employed to guarantee the thorough PHY evaluation on IEEE 802.11p and IEEE 802.11bd. Secondly, to remedy the incomplete analysis on antenna configurations in which the SISO channel is the single configuration considered in numerous existing studies, the various multi-antenna configurations, including the MIMO, SIMO, and MISO systems, are combined with the SISO system to fully investigate the difference between the multi-antenna and single-antenna configurations. Finally, to deeply uncover the impact of each parameter on the PHY performance which cannot be found in the fixed parameter or slightly different parameters utilized in some prior research, the considerably different packet sizes and MCSs are discussed by means of the ultra-reliable low-latency communications (URLLC) application and enhanced mobile broadband (eMBB) application with the low MCS and high MCS for the urban NLOS and highway NLOS channel models under the V2V scenarios.

CHAPTER THREE

THEORIES AND TECHNOLOGIES

3.1 OSI Model

In the OSI model of the computer networking, the communications between systems are split into seven different abstraction layers, including physical layer, data link layer, network layer, transport layer, session layer, presentation layer, and application layer, from bottom to top with bit, frame, packet, segment, data, data, and data as the protocol data unit (PDU) respectively, as shown in Fig. 3.1 where the host layers and the media layers are indicated. Each layer in the OSI model has well-defined functions, and each intermediate layer can communicate and interact with those layers immediately above and below it.

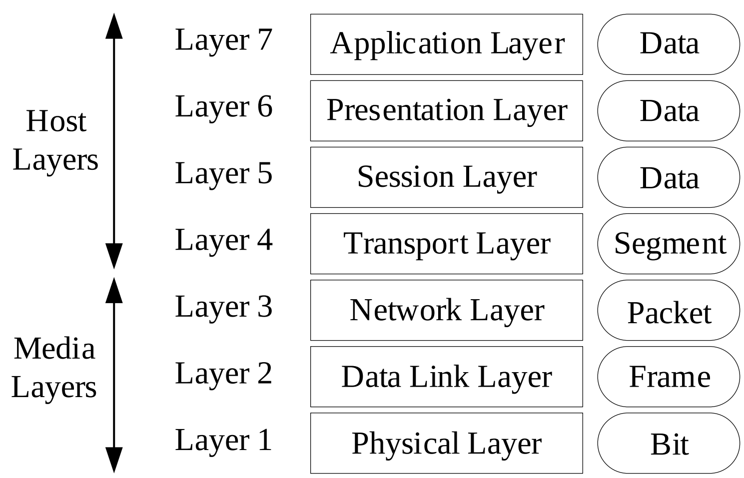

Figure 3.1 OSI model

3.1.1 Physical Layer

The physical layer, the first and lowest layer which is most closely associated with the physical connection between devices, is responsible for the transmission and reception of unstructured raw data between a device and a physical transmission medium. It converts the digital bits into electrical, radio, or optical signals, and defines the connector, the electrical cable or wireless technology connecting the devices.

3.1.2 Data Link Layer

The data link layer encodes, decodes, and organizes data bits between two adjacent nodes on the same local area network (LAN) or wide area network (WAN). It is divided into two sublayers, i.e., the MAC sublayer and the logical link control (LLC) sublayer. The lower MAC sublayer defines rules for accessing the common medium so that it can be shared efficiently and fairly among a set of stations (STAs). The upper LLC sublayer provides multiplexing mechanisms that make it possible for several network protocols to coexist within a multipoint network and to be transported over the same network medium. It can also provide flow control and automatic repeat request (ARQ) error management mechanisms.

3.1.3 Network Layer

The network layer handles routing of data from the source to the destination, multi-hop broadcast communications for the decentralized environmental notification messages (DENMs), and data dissemination to a particular geographical area.

3.1.4 Transport Layer

The transport layer provides services such as end-to-end delivery, reliable data transfer, and congestion mitigation.

3.1.5 Session Layer

The session layer is responsible for establishing, maintaining, synchronizing, and terminating sessions between end-user applications.

3.1.6 Presentation Layer

The presentation layer extracts and manipulates the data from the application layer as per the required format to transmit over the network.

3.1.7 Application Layer

The application layer defines various types of messages that are used by vehicles to enable the ITS applications, including message formats, message coverage range, and message inter-arrival times [38]. For safety applications, periodic messages known as the cooperative awareness messages (CAMs) and the basic safety messages (BSMs) are transmitted by vehicles [38]. For non-safety applications, the event-driven DENMs are shared by vehicles [38].

The upper layers, including the application layer, presentation layer, session layer, transport layer, and network layer, of the protocol stack are shared by both the DSRC and the C-V2X, whereas the MAC and PHY layers are different in both technologies. Utilizing the Wi-Fi-based access technology, the DSRC is suitable for the short-range communications but does not provide robust connectivity for the high vehicle density [38]. On the other hand, employing the cellular-based access technology, the C-V2X can support a longer coverage range, but its direct communication transmission mode cannot provide the desired high reliability [38].

3.2 DSRC

The DSRC is a standard proposed by the FCC which is deployed on the allocated $75\ \text{MHz}$ bandwidth in the $5.9\ \text{GHz}$ frequency band, $5.850-5.925\ \text{GHz}$, to support the V2V, V2I, and V2P communications. A DSRC system which consists of an on-board unit (OBU) and a road-side unit (RSU) can realize a short-range communication with a coverage of hundreds of meters [3].

The DSRC spectrum is divided into seven $10\ \text{MHz}$ channels with a $5\ \text{MHz}$ guard band at the low end reserved to prevent interference. Channel 178, $5.885-5.895\ \text{GHz}$, is the control channel (CCH) assigned for the transmission of control messages, such as the WAVE Service Advertisement (WSA) messages, and for safety applications [12]. It is the unique channel shared between all the WAVE devices and constitutes a joining point between the nodes [3]. The remaining channels are service channels (SCHs) intended for general-purpose application data transfers. Channels 172 and 184 are designated for public safety applications involving safety of life and property [25]. Specifically, channel 172 is dedicated for the V2V safety communications for accident avoidance and mitigation, and safety of life and property applications and channel 184 is exclusively for high-power and longer-distance communications in public safety applications [25]. Meanwhile, channels 174 and 176 are designed as medium-power service channels, whereas channels 180 and 182 are low-power service channels [12]. Pairs of these adjacent $10\ \text{MHz}$ channels can be combined into a $20\ \text{MHz}$ channel, thus channels 174 and 176 and channels 180 and 182 are combined to produce channels 175 and 181 respectively. However, based on the requirement to support many parallel types of applications, and on the physical testing which suggests the suitability of the

10 MHz bandwidth to the delay spread and Doppler spread encountered in the vehicular environment, testing of the DSRC in the U.S. has focused on 10 MHz channels [39]. Furthermore, the 20 MHz channel has more noise for a given background spectral density and may pose a greater challenge for some environments, e.g., inter-symbol interference (ISI) due to a delay spread that exceeds the shortened cyclic prefix (CP) length [39]. The channel allocation in the DSRC spectrum is demonstrated in Fig. 3.2 [25].

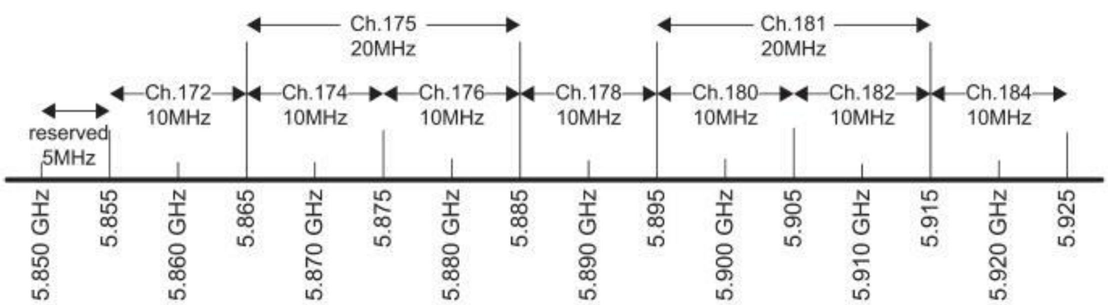

Figure 3.2 DSRC channel allocation

In the DSRC protocol architecture, the specific protocol is applied to each layer. The IEEE 802.11p is a modified version of the familiar IEEE 802.11 standard for Wi-Fi and adopted in the PHY and MAC layers. A suite of standards defined by the IEEE 1609 Working Group (WG) are employed in the middle of the stack. Specifically, the IEEE 1609.2, 1609.3, and 1609.4 protocols are utilized for security services, network services including the WAVE Short Message Protocol (WSMP), and channel switching respectively

[3][39][40]. In addition to the WSMP, the other Internet protocols, including the Internet Protocol version 6 (IPv6), User Datagram Protocol (UDP), and Transmission Control Protocol (TCP), are also supported by the DSRC for the network and transport layers [39]. The choice between using the WSMP or IPv6+UDP/TCP depends on the requirements of a given application. Single-hop messages, like those upon which the collision-prevention applications are based, typically utilize the bandwidth-efficient WSMP which is optimized for the non-routed data exchanges that are common to vehicular networks, e.g., the V2V safety messages, while multi-hop packets employ IPv6 for its routing capability [39].

Moreover, the SAE J2735 DSRC Message Set Dictionary standard defines fifteen messages that collectively enable a core set of the DSRC applications, and specifies their data elements and data frames, for various vehicle-based applications [3][39]. As the most important message, the BSM conveys critical vehicle state information in support of the V2V safety applications. The BSM transmission rate and power, accuracy of the BSM data elements, and channel congestion control are to be addressed in the SAE J2945.1 communication minimum performance requirements standard [39].

The detailed protocol stack in the DSRC architecture introduced above is illustrated in Fig. 3.3 [3][39].

3.2.1 IEEE 802.11p

As an improved IEEE 802.11 protocol completed in 2010, IEEE 802.11p is used to describe the PHY and MAC layers for interchanging wireless broadcast messages in a vehicular environment with the allocation of the $75\ \text{MHz}$ bandwidth at the $5.850-5.925\ \text{GHz}$ frequency band. By halving the channel bandwidth from $20\ \text{MHz}$ to $10\ \text{MHz}$ and increasing the carrier frequency from $5\ \text{GHz}$ to $5.9\ \text{GHz}$, with all the corresponding doubled timing OFDM parameters, the IEEE 802.11p was extended from IEEE 802.11a, which was designed for the short-range, low-mobility, and indoor applications, to meet the requirements on the longer range, extreme-high mobility, and rapid-changing channel conditions [4].

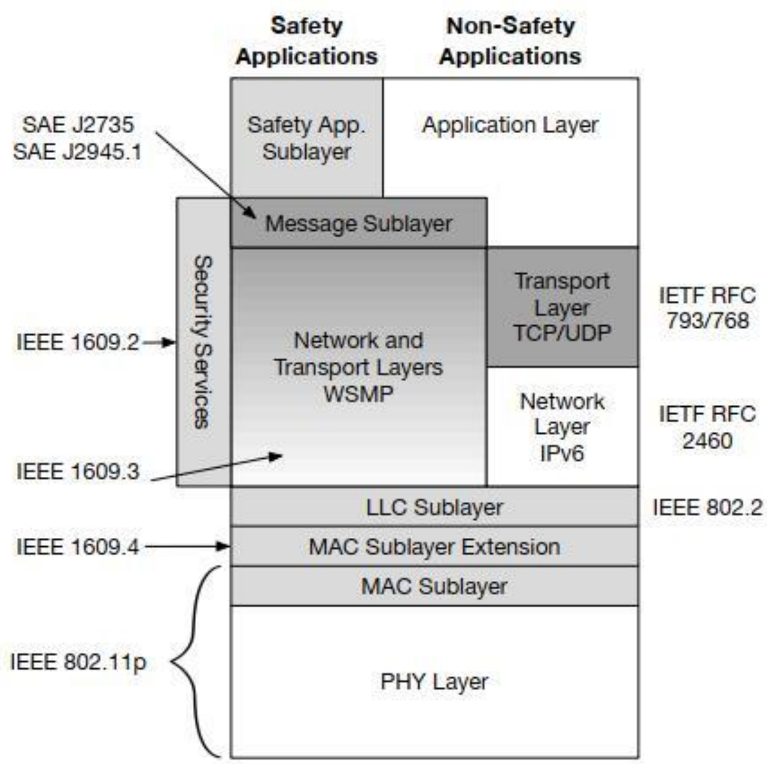

Figure 3.3 DSRC protocol architecture

The PHY parameters of IEEE 802.11p compared with IEEE 802.11a are listed in Table 3.1 [9][41] where the OFDM symbol duration is provided with the guard interval (GI) included.

Table 3.1 PHY comparison between IEEE 802.11a and IEEE 802.11p

Parameter	IEEE 802.11a	IEEE 802.11p
Data Subcarriers	48	48
Pilot Subcarriers	4	4
Null Subcarriers	12	12
Total Subcarriers	64	64
Channel Bandwidth	20 MHz	10 MHz
Subcarrier Spacing	20 MHz/64=312.5 KHz	10 MHz/64=156.25 KHz
OFDM Symbol Duration	4 μs (800 ns GI)	8 μs (1.6 μs GI)

In the OFDM PHY of IEEE 802.11p, the PHY protocol data unit (PPDU), which is the unit of data exchanged between two peer PHY entities to provide the PHY data service, includes the PHY Preamble field, SIGNAL field, and DATA field. Specifically, the PHY Preamble field consists of 10 short training symbols denoted as $t_i (i = 1, 2, \cdots, 10)$ and 2 long training symbols denoted as $T_i (i = 1, 2)$; the SIGNAL field is a single OFDM symbol; and the DATA field may constitute multiple OFDM symbols. The PPDU format, Preamble field, SIGNAL field, and DATA field of IEEE 802.11p are demonstrated in Fig. 3.4, Fig. 3.5, Fig. 3.6, and Fig. 3.7 respectively [9][41] where T_{STF}, T_{LTF}, T_{PREAMBLE}, T_{SIGNAL}, and T_{DATA} represent the duration of the Short Training field (STF), Long Training field (LTF), Preamble field, SIGNAL field, and DATA field respectively and GI2 is the double guard interval.

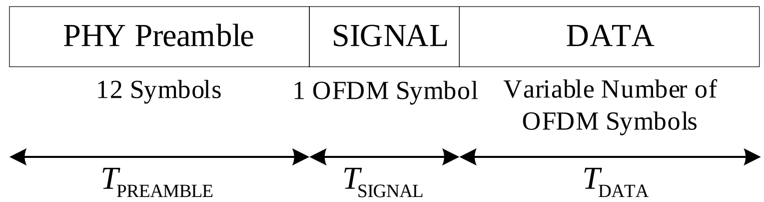

Figure 3.4 PPDU format of IEEE 802.11p

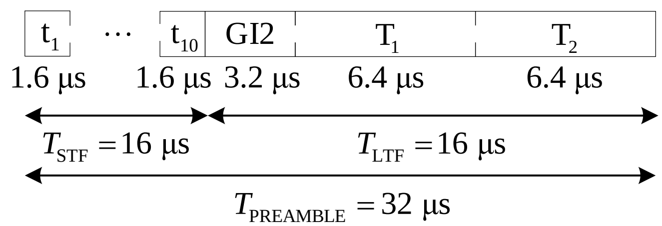

Figure 3.5 Preamble field of IEEE 802.11p

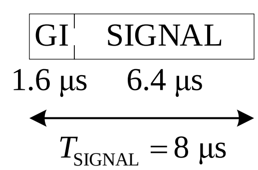

Figure 3.6 SIGNAL field of IEEE 802.11p

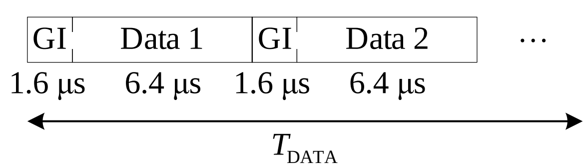

Figure 3.7 DATA field of IEEE 802.11p

Depending on the distance between the transmitter and the receiver, the channel conditions, and the quality of service (QoS) requirements, an appropriate MCS should be selected for the efficient transmission from eight candidate MCSs which are indexed from 0 to 7 as outlined in Table 3.2 [9].

3.2.2 IEEE 802.11bd

Aimed at improving the communication reliability, transmission range, and throughput compared to the legacy IEEE 802.11p standard, IEEE 802.11bd was proposed as the NGV standard which defines modifications to both the IEEE 802.11 PHY and MAC layers for the V2X communications in the 5.9 GHz frequency band and optionally in the 60 GHz band [42]. The advancements are expected to achieve at least twice the MAC throughput of IEEE 802.11p with relative speeds up to 500 km/h, at least 3 dB lower sensitivity level and thus twice the communication range of IEEE 802.11p, and interoperability, coexistence, backward compatibility, and fairness with IEEE 802.11p devices [1][38][42].

In comparison with the Wi-Fi standards which have been developed for the low-mobility applications, the DSRC was designed for the high-mobility vehicular networks and the corresponding enhancements were introduced to make the DSRC suitable for such environments [1]. Since 20 MHz IEEE 802.11ac OFDM numerology is shown as a good choice for 10 MHz DSRC channel for its efficiency and Doppler resilience [10], the bandwidth of IEEE 802.11bd is reduced to 10 MHz by halving the 20 MHz bandwidth of IEEE 802.11ac and thus all the OFDM timing parameters are doubled in order to make the signal more robust against fading and more tolerant to multipath effects in the vehicular environment.

Table 3.2 MCS options, data rates, and transmission latencies of IEEE 802.11p

MCS	Modulation	Coding Rate	Theoretical Data Rate (Mbps)	Actual Data Rate (Mbps)		Transmission Latency (ms)	
				100 bytes	1500 bytes	100 bytes	1500 bytes
0	BPSK	1/2	3.00	2.33	2.95	0.344	4.07
1	BPSK	3/4	4.50	3.13	4.37	0.256	2.74
2	QPSK	1/2	6.00	3.85	5.79	0.208	2.07
3	QPSK	3/4	9.00	4.76	8.52	0.168	1.41
4	16-QAM	1/2	12.00	5.56	11.19	0.144	1.07
5	16-QAM	3/4	18.00	6.67	16.13	0.120	0.744
6	64-QAM	2/3	24.00	7.14	20.83	0.112	0.576
7	64-QAM	3/4	27.00	7.69	23.08	0.104	0.520

The comparison on the PHY parameters between IEEE 802.11ac and IEEE 802.11bd is shown in Table 3.3 [9][14] where the OFDM symbol duration is provided with the GI included.

In addition to a preamble located at the beginning of a frame which is used for the initial channel estimation, midambles, which are introduced in between the OFDM data symbols periodically, will help in channel tracking so that accurate channel estimates are obtained for all data symbols [1]. With the channel update based on an appropriate periodicity of midambles, the fast variation of the channel can be limited within each midamble periodicity and the PER at the receiver can be effectively decreased [10]. Although the denser midambles can lead to better channel estimation and lower PER, the throughput will also be reduced since the packet duration is increased with the more frequent insertion of midambles [26]. Hence, the midamble periodicity should be properly determined from three candidates, 4, 8, and 16 OFDM symbols [11], in terms of modulation, error control, Doppler spread, and so on [1]. Moreover, the low-density parity-check (LDPC) coding is exploited as the forward error correction (FEC) coding technique to replace the binary convolutional coding (BCC) in IEEE 802.11p [38]. With the combination of the midamble and the LDPC, the prominent signal-to-noise ratio (SNR) gain and Doppler mitigation can be achieved [10].

Table 3.3 PHY comparison between IEEE 802.11ac and IEEE 802.11bd

PHY Parameter	IEEE 802.11ac	IEEE 802.11bd
Data Subcarriers	52	52
Pilot Subcarriers	4	4
Null Subcarriers	8	8
Total Subcarriers	64	64
Channel Bandwidth	20 MHz	10 MHz
Subcarrier Spacing	20 MHz/64=312.5 KHz	10 MHz/64=156.25 KHz
OFDM Symbol Duration	4 μs (800 ns GI), 3.6 μs (400 ns GI)	8 μs (1.6 μs GI)

In the NGV PHY of IEEE 802.11bd, the NGV PPDU format includes the NGV Preamble field and NGV DATA field. Specifically, the NGV Preamble field contains non-high-throughput (HT) Short Training field (L-STF), non-HT Long Training field (L-LTF), non-HT SIGNAL field (L-SIG), repeated L-SIG (RL-SIG), NGV SIGNAL field (NGV-SIG), repeated NGV-SIG (RNGV-SIG), NGV Short Training field (NGV-STF), and NGV Long Training field (NGV-LTF); meanwhile, the NGV DATA field involves the OFDM data symbols with the midambles inserted after every M data symbols when the midamble periodicity is specified as M .

The NGV PPDU format, NGV Preamble field, and NGV DATA field of 10 MHz IEEE 802.11bd are illustrated in Fig. 3.8, Fig. 3.9, and Fig. 3.10 respectively [11][14][36] where T_{PREAMBLE} and T_{DATA} represent the duration of the NGV Preamble field and NGV DATA field respectively and L satisfies $L < M$.

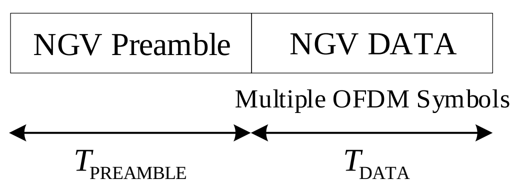

Figure 3.8 NGV PPDU format of IEEE 802.11bd

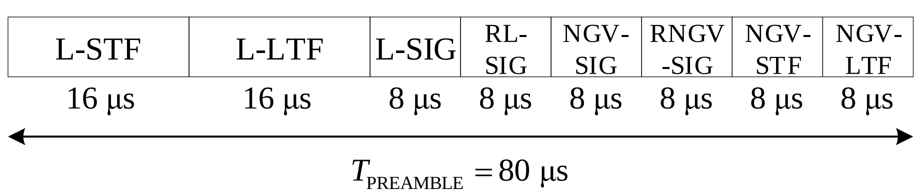

Figure 3.9 NGV Preamble field of IEEE 802.11bd

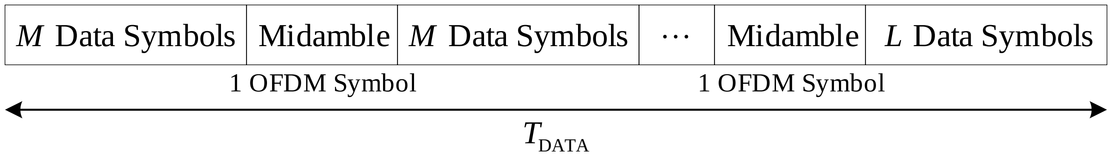

Figure 3.10 NGV DATA field of IEEE 802.11bd

The MCS 0-8 of 10 MHz IEEE 802.11bd can be derived from 20 MHz IEEE 802.11ac, whereas MCS 15 is the same as MCS 0 except that the dual carrier modulation (DCM) mode is adopted [6][14]. By means of the receiver distance, the channel conditions, and the QoS requirements, one proper MCS is selected for the efficient transmission from all the possible MCSs indexed from 0 to 15 which are summarized in Table 3.4 [11][14] where the midamble periodicity is specified as 4 OFDM symbols for all MCSs to obtain the best reliability at the expense of the throughput. Furthermore, MCS 9 of 10 MHz IEEE 802.11bd is not valid since the number of data bits per OFDM symbol is not an integer. Moreover, MCS 10-14 are reserved for future application.

3.3 LOS and NLOS Propagation

In contrast to the LOS propagation where there exists direct path travelling from the transmitter to the receiver which experiences the shortest possible distance [43], the NLOS propagation occurs when there are obstacles existing which block the direct communication but preserve the indirect communication between the transmitter and receiver. Both the LOS and NLOS propagation are demonstrated in Fig. 3.11 [44].

Table 3.4 MCS options, data rates, and transmission latencies of 10MHz IEEE 802.11bd

MCS	Modulation	Coding Rate	Theoretical Data Rate (Mbps)	Actual Data Rate (Mbps)		Transmission Latency (ms)	
				100 bytes	1500 bytes	100 bytes	1500 bytes
0	BPSK	1/2	3.250	1.923	2.538	0.416	4.728
1	QPSK	1/2	6.500	3.030	4.967	0.264	2.416
2	QPSK	3/4	9.750	3.704	7.282	0.216	1.648
3	16-QAM	1/2	13.00	4.348	9.494	0.184	1.264
4	16-QAM	3/4	19.50	4.762	13.64	0.168	0.880
5	64-QAM	2/3	26.00	5.556	17.44	0.144	0.688
6	64-QAM	3/4	29.25	5.556	19.23	0.144	0.624
7	64-QAM	5/6	32.50	5.556	20.83	0.144	0.576
8	256-QAM	3/4	39.00	5.882	24.19	0.136	0.496
9	Not valid						
10-14	Reserved						
15	BPSK-DCM	1/2	1.625	1.099	1.284	0.728	9.344

There are three dominant radio-propagation mechanisms which embrace reflection, diffraction, and scattering when faced with obstacles in wireless communications as shown in Fig. 3.12 [43][45]. When the radio wave propagating in one medium impinges upon another medium which is larger than the wavelength of the radio signal, the radio wave is reflected off the surface and thus reflection occurs. Diffraction arises when the propagating radio wave is blocked by an object with sharp irregular edges and then bends around the corners of the object. Scattering happens when the radio wave hits a rough surface or an object which is much smaller than the wavelength and then bounces off in multiple directions.

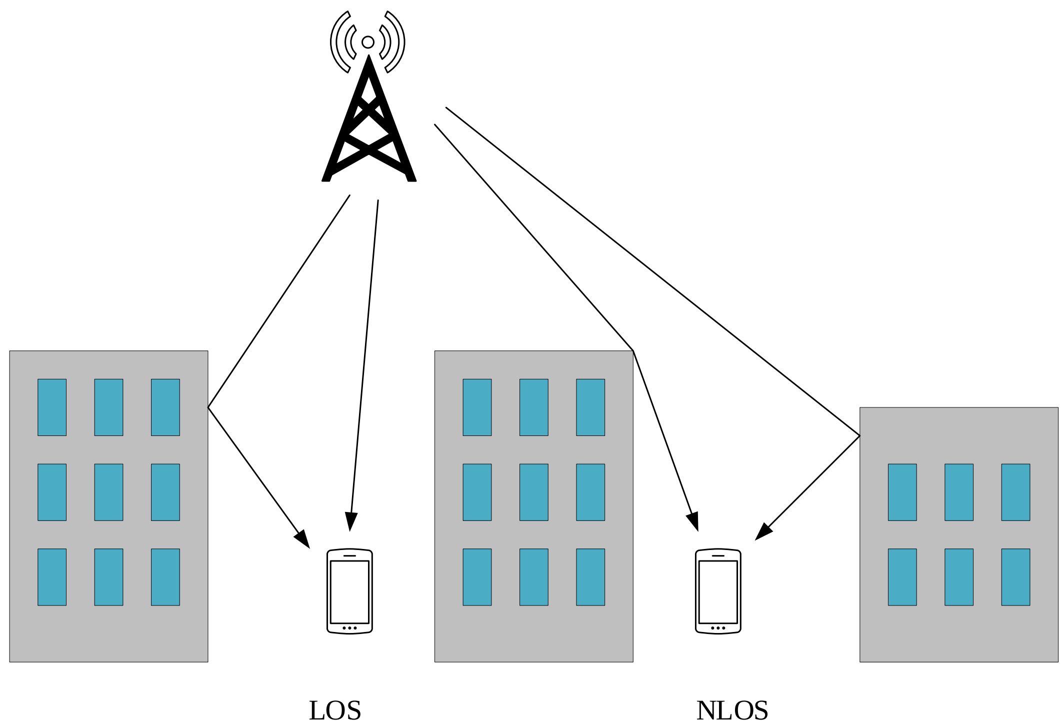

Figure 3.11 LOS and NLOS propagation

Along the multiple paths generated in the reflection, diffraction, and scattering mechanisms induced by the encounter with the obstacles, the fluctuation on power of the received signal takes place in space, and/or in frequency, and/or in time, due to angle spread, delay spread, and Doppler spread respectively, according to the random superposition of all multipath components [46][47]. As a result, in addition to scarce available bandwidth, path loss, co-channel interference, and noise which are the typical impairments in the LOS propagation of the wireless channel, the other impairments, for example, the multipath fading that is composed of the severe fluctuations in the received signal, also exist during the NLOS propagation [46][48].

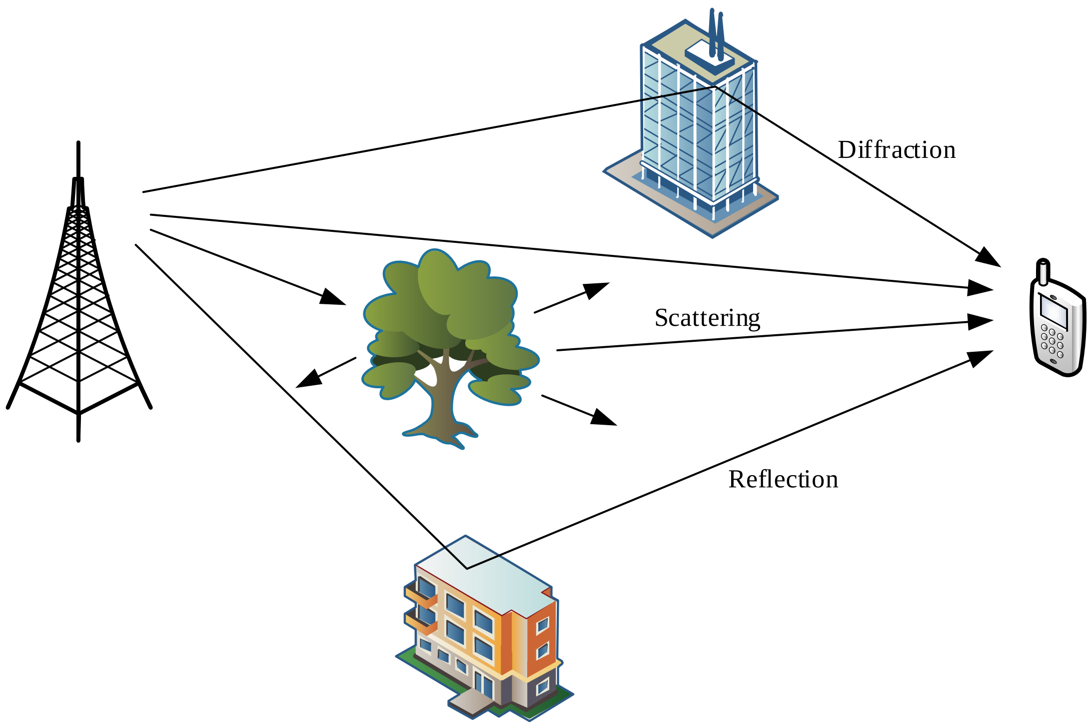

Figure 3.12 Reflection, diffraction, and scattering

Based on the multipath taps over which the direct signal and the reflected/diffracted/scattered signals are characterized by the power, root mean square (RMS) delay spread, and Doppler spread obtained by various measurements for usual V2V scenarios, the performance evaluation can be fulfilled on the V2V radio channel models which are established for the rural LOS, urban approaching LOS, urban crossing NLOS, highway LOS, and highway NLOS scenarios respectively [49].

With more rich multipath components, the NLOS propagation suffers from the more serious multipath fading which is challenging for the desired high-performance communications. However, the multi-antenna systems can leverage the multipath effect to improve the performance of wireless communications and thus generate more significant promotion in the NLOS propagation than in the LOS propagation [50]. Accordingly, the urban NLOS and highway NLOS channel models provided in [49] instead of the LOS channel models are analyzed in the simulation to explicitly demonstrate the superiority of the multi-antenna configurations.

3.4 V2V Channel Model

Various measurement results obtained in three existing studies for the general V2V scenarios were involved and merged by the IEEE 802.11 DSRC group in [49], which include the rural LOS scenario, urban approaching LOS scenario, urban crossing NLOS scenario, highway LOS scenario, and highway NLOS scenario, as shown in Fig. 3.13, Fig. 3.14, Fig. 3.15, Fig. 3.16, and Fig. 3.17 respectively. Characterized by the statistics of a suite of the power, RMS delay spread, and Doppler spread, the realistic scenarios investigated constitute the baseline for the V2V radio channel models.

3.4.1 Rural LOS Scenario

In an open environment without other vehicles, buildings, and large fences, the LOS communication is dominant between vehicles with several weak multipath components present. The maximum speed difference between the paths is $144\ \text{km/h}$.

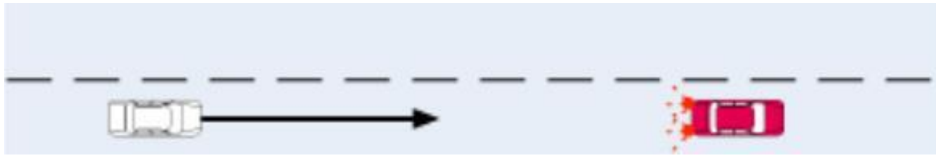

Figure 3.13 Rural LOS scenario

3.4.2 Urban Approaching LOS Scenario

Based on the communication between two approaching vehicles in an urban street with surrounding buildings, the multipath components become stronger compared to the rural LOS scenario but remain weaker than the LOS component. The maximum speed difference between the paths is 119 km/h .

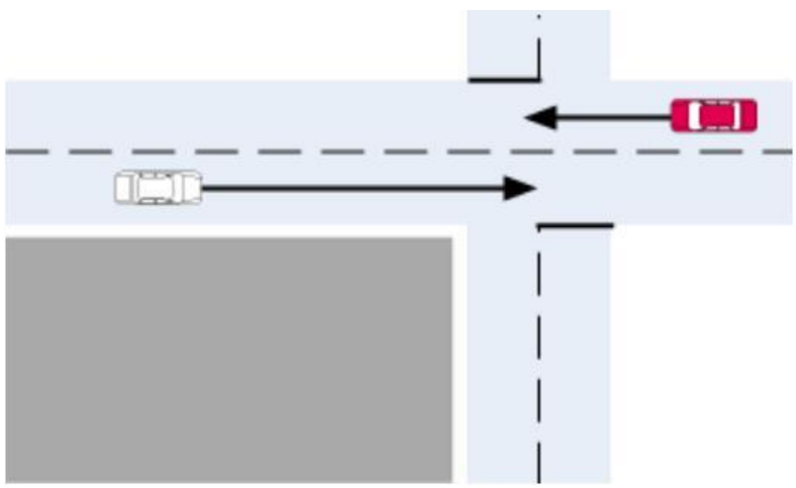

Figure 3.14 Urban approaching LOS scenario

3.4.3 Urban Crossing NLOS Scenario

As two vehicles approach an urban blind intersection with other traffic, buildings, and fences, the NLOS communication becomes predominant due to the much stronger multipath components and the strong fading occurs with the absence of dominant LOS component as well as the small difference on power in the multipath components [37]. The maximum speed difference between the paths is $126\ \text{km/h}$.

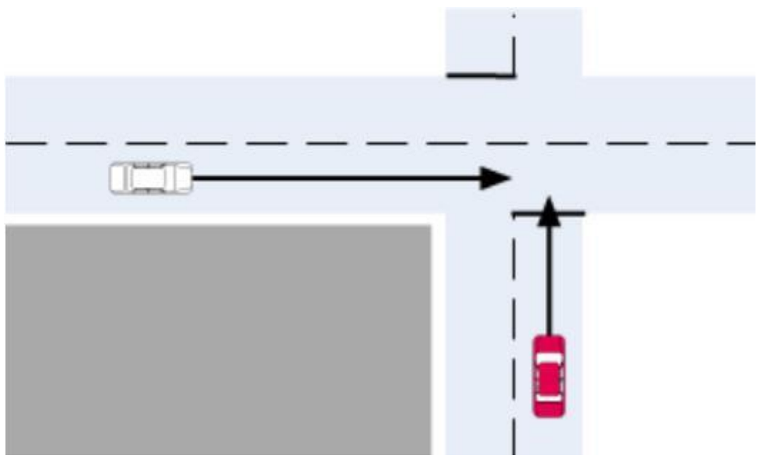

Figure 3.15 Urban crossing NLOS scenario

3.4.4 Highway LOS Scenario

During the communication between two vehicles following each other on the multilane inter-region roadways with the signs, overpasses, hillsides, and other traffic, the remarkable LOS communication is accompanied by a higher Doppler shift which is generated with the higher differential speed between vehicles. The maximum speed difference between the paths is $252\ \text{km/h}$.

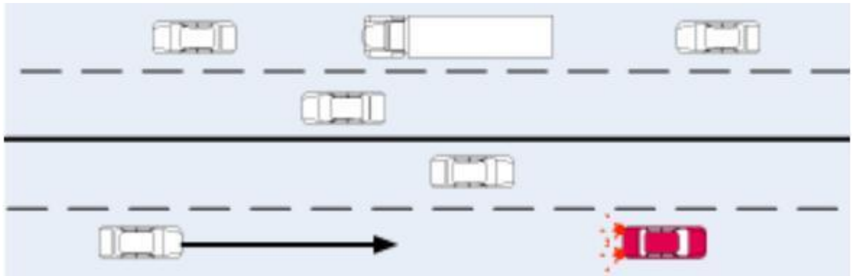

Figure 3.16 Highway LOS scenario

3.4.5 Highway NLOS Scenario

When a truck is in between communicating vehicles and blocking the LOS path compared to the highway LOS scenario, the NLOS communication is significant with the much stronger multipath components and the fast fading arises due to the high Doppler spread [37]. The maximum speed difference between the paths is $252\ \mathrm{km/h}$.

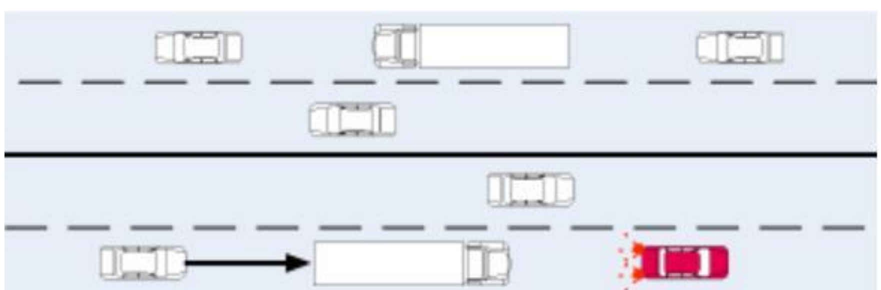

Figure 3.17 Highway NLOS scenario

Based on the five investigated V2V scenarios, the V2V radio channel models are proposed for the PHY performance evaluation and testing under the time-selective and frequency-selective propagation conditions [26], as described in [49]. The corresponding parameters of the V2V channel models are listed in Table 3.5 where the power in dB, RMS delay spread in ns, and Doppler spread in Hz of the direct path and several dominant indirect paths for each scenario are specified.

Table 3.5 V2V channel model parameters

V2V Scenario	Power (dB)	RMS Delay Spread (ns)	Doppler Spread (Hz)
Rural LOS	[0 -14 -17]	[0 83 183]	[0 492 -295]
Urban Approaching LOS	[0 -8 -10 -15]	[0 117 183 333]	[0 236 -157 492]
Urban Crossing NLOS	[0 -3 -5 -10]	[0 267 400 533]	[0 295 -98 591]
Highway LOS	[0 -10 -15 -20]	[0 100 167 500]	[0 689 -492 886]
Highway NLOS	[0 -2 -5 -7]	[0 200 433 700]	[0 689 -492 886]

3.5 OFDM and MIMO

3.5.1 OFDM Modulation Scheme

In the wireless communications where the reflection, diffraction, and scattering are the dominant radio-propagation mechanisms, the delay spread is caused by the multipath propagation and the ISI is generated because of the time dispersion in the wireless channel [43][45]. According to the OFDM modulation scheme employed on the IEEE 802.11p and IEEE 802.11bd PHY, the entire wide-band channel over which the high-rate data stream is transmitted is partitioned into multiple narrow-band subchannels whose bandwidth is smaller than the channel coherence bandwidth [51][52]. Hence, the frequency-selective-fading channel is transformed into many flat-fading subchannels which are more robust against the multipath fading [52][53][54][55]. Based on the parallel transmission over the overlapping orthogonal subcarriers which provides the high spectral efficiency [6][56], the high-data-rate transmission can be guaranteed, meanwhile, the symbol duration can be increased to alleviate the time dispersion and the resulting ISI in the multipath channel [54][57][58][59].

A CP is appended to one OFDM symbol by replicating a segment from the end of the OFDM symbol to the beginning of the symbol [60], and the duration of the CP should be longer than the maximum delay spread to mitigate the ISI in the multipath channel [52][54][59][61]. With the cyclic extension of the OFDM symbol, the linear convolution between the transmitted signal and the channel impulse response in the single-carrier system is converted into the circular convolution in the multi-carrier system which is significant to maintain the subcarrier orthogonality [52][53][62]. Accordingly, compared to the single-carrier system which requires the complex time-domain equalizer, the simpler per-subcarrier equalizer is performed in the frequency domain for the multi-carrier system to offset the distortion induced by the channel [54][59][62][63].

Since there are 64 subcarriers included in a single OFDM symbol of IEEE 802.11p and IEEE 802.11bd, a 64-point inverse fast Fourier transform (IFFT) performed at the OFDM modulator in the transmitter and a 64-point fast Fourier transform (FFT) at the OFDM demodulator in the receiver are combined so that the efficient implementation integrated into the commercial hardware can be guaranteed [59][62][64].

The architecture of the OFDM modulation scheme is described in Fig. 3.18 [52][59][62][65] where S/P and P/S represent the serial-to-parallel convertor and parallel-to-serial convertor respectively.

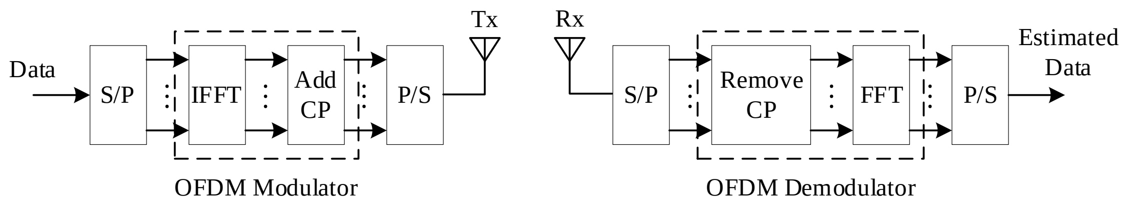

Figure 3.18 OFDM modulation scheme

3.5.2 Multi-antenna Configurations

According to the deployment of multiple antennas on one side or both sides of the communication link, the multi-antenna configurations, which contain the MIMO, SIMO, and MISO, can improve the bit error rate (BER) or data rate without consuming any additional transmit power and bandwidth compared to the SISO configuration [52][57][66][67]. Instead of combating the multipath property of the wireless channel, the MIMO, SIMO, and MISO systems exploit the multipath to increase the SNR and thus the channel capacity, and to improve the reliability, coverage, and throughput by sharing the communication resources not only in the time and frequency domain, but also in the space domain [51][59].

Three multi-antenna techniques, which include spatial diversity, spatial multiplexing, and beamforming, are respectively utilized to obtain the diversity gain, multiplexing gain, and array gain [51][52][66], in which there is a trade-off strategy between the diversity gain and the multiplexing gain to accommodate the specific requirement for different applications [52][68].

The MIMO system model which is composed of N_{T} transmit antennas and N_{R} receive antennas is demonstrated in Fig. 3.19 [46][51][68].

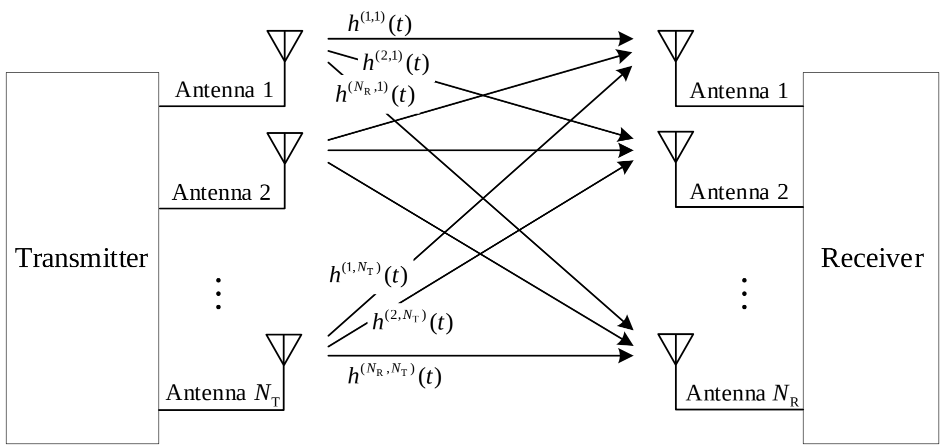

Figure 3.19 MIMO system model

As a result of the linearity of the propagation environment, the *j*th receive antenna observes the superposition [65]

$$y^{(j)}(t) = \sum_{i=1}^{N_{\mathrm{T}}} \int_{-\infty}^{\infty} h^{(j,i)}(\tau) x^{(i)}(t-\tau) d\tau + v^{(j)}(t), \quad j = 1, \cdots, N_{\mathrm{R}} \tag{3.1}$$

where $x^{(i)}(t)$ is the signal transmitted by the ith transmit antenna, $h^{(j,i)}(t)$ is the impulse response between the ith transmit antenna and the jth receive antenna, and $v^{(j)}(t)$ is the additive white Gaussian noise (AWGN) at the jth receive antenna which is independent of the noise from the other receive antennas.

The $N_{\mathrm{R}} \times 1$ received signal vector and noise vector are respectively expressed as

$$\mathbf{y}(t) = \begin{bmatrix} y^{(1)}(t) \\ \vdots \\ y^{(N_{\mathrm{R}})}(t) \end{bmatrix} \tag{3.2}$$

and

$$\mathbf{v}(t) = \begin{bmatrix} v^{(1)}(t) \\ \vdots \\ v^{(N_{\mathrm{R}})}(t) \end{bmatrix}. \tag{3.3}$$

The $N_{\mathrm{T}} \times 1$ transmitted signal vector is expressed as

$$\mathbf{x}(t) = \begin{bmatrix} x^{(1)}(t) \\ \vdots \\ x^{(N_{\mathrm{T}})}(t) \end{bmatrix}. \tag{3.4}$$

The $N_{\mathrm{R}} \times N_{\mathrm{T}}$ normalized channel matrix is expressed as [69]

$$\mathbf{H}(t) = \begin{bmatrix} h^{(1,1)}(t) & h^{(1,2)}(t) & \cdots & h^{(1,N_{\mathrm{T}})}(t) \\ h^{(2,1)}(t) & h^{(2,2)}(t) & \cdots & h^{(2,N_{\mathrm{T}})}(t) \\ \vdots & \vdots & \ddots & \vdots \\ h^{(N_{\mathrm{R}},1)}(t) & h^{(N_{\mathrm{R}},2)}(t) & \cdots & h^{(N_{\mathrm{R}},N_{\mathrm{T}})}(t) \end{bmatrix}. \tag{3.5}$$

The continuous received signal of the MIMO system can be expressed as [65]

$$\mathbf{y}(t) = \int_{-\infty}^{\infty} \mathbf{H}(\tau)\mathbf{x}(t-\tau)d\tau + \mathbf{v}(t), \tag{3.6}$$

where $\mathbf{y}(t)$ is the $N_\mathrm{R} \times 1$ received signal vector, $\mathbf{H}(t)$ is the $N_\mathrm{R} \times N_\mathrm{T}$ normalized channel matrix, $\mathbf{x}(t)$ is the $N_\mathrm{T} \times 1$ transmitted signal vector, and $\mathbf{v}(t)$ is the $N_\mathrm{R} \times 1$ noise vector, respectively.

The discrete received signal of the MIMO system can be expressed as [65][70]

$$\mathbf{y}[n] = \sum_{l=0}^{L} \mathbf{H}[l]\mathbf{x}[n-l] + \mathbf{v}[n], \tag{3.7}$$

where $\mathbf{y}[n]$, $\mathbf{H}[n]$, $\mathbf{x}[n]$, and $\mathbf{v}[n]$ are the received signal vector, normalized channel matrix, transmitted signal vector, and noise vector, which have been discretized respectively.

If the channel tap number L is equal to 0, the input-output relationship on the flat-fading MIMO channel can be derived from the reduction of the frequency-selective-fading MIMO channel and expressed as [65][71][72][73]

$$\mathbf{y}[n] = \mathbf{H}\mathbf{x}[n] + \mathbf{v}[n]. \tag{3.8}$$

The MIMO systems can be used either to realize reliable communication by sending the multiple copies of the same bit stream over independent paths in the spatial diversity or to increase the data transmission rate by sending the different bit streams in parallel in the spatial multiplexing [40][74]. To compromise between maximizing the diversity gain to increase the link reliability against fading and maximizing the multiplexing gain to achieve the best spectral efficiency, the trade-off between the diversity gain and the multiplexing gain needs to be exploited [68].

The multiplexing gain r satisfies the relationship with [68][75][76]

$$0 \le r \le \min(N_\mathrm{T}, N_\mathrm{R}), \tag{3.9}$$

then the optimal diversity gain can be calculated as [68][75][76]

$$d_{\text{opt}}(r) = (N_{\text{T}} - r)(N_{\text{R}} - r). \tag{3.10}$$

3.5.3 MIMO-OFDM Scheme

Since most of the MIMO techniques are explored for the flat-fading channel, the OFDM scheme which provides the narrowband flat-fading channel can be integrated into the MIMO technique to support the transmission over the wideband frequency-selective-fading channel [52][58][63][66]. Each subcarrier can be modeled as an independent MIMO system in the OFDM-based transmission, consequently, the MIMO-OFDM receiver can be simplified due to the operation on the independent subcarriers when the CP is long enough to eliminate the time dispersion of the multipath channel [59].

Different from the transmitted signals generated from the OFDM transmitter which can only be constructed within a symbol-subcarrier grid on the time-frequency plane, the output signals of the MIMO encoder can be represented in either space-time plane, or space-frequency plane, or space-time-frequency plane in the MIMO-OFDM system by virtue of the introduction of a third spatial dimension which provides more implementation flexibility [53]. Based on the combination of the OFDM scheme and the MIMO technique, the high-speed wireless communications can be maintained by taking advantage of the benefits of both technologies with the further improved performance [53][66].

The architecture of the MIMO-OFDM scheme with N_{T} transmit antennas and N_{R} receive antennas is portrayed in Fig. 3.20 [53][59][65][66].

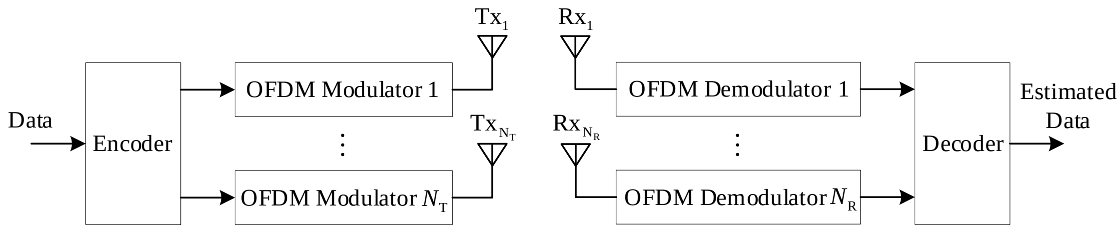

Figure 3.20 MIMO-OFDM scheme

3.6 PHY Metrics

3.6.1 PER

To describe the communication reliability which represents the receiver performance, the PER is defined as the most usual PHY metric which is the percentage of the erroneously received packets to the total transmitted packets [6][31][46]. As a function of the transmitted SNR with a logarithmic scale, the lower PER corresponds to the higher reliability of communication.

3.6.2 PRR

Contrary to the definition of the PER, the PRR refers to the percentage of the successfully received packets to the total transmitted packets which indicates the likelihood of successful transmissions [6][31][46]. As a function of the distance between the transmitter and receiver in a non-logarithmic scale, the higher PRR implies the higher possibility of successful communication and thus the higher reliability of the link. Transmission coverage, which is utilized to measure the maximum communication range, is defined as the transmission distance at which the desired link-level PRR, such as 90%, can be met to satisfy the rigorous requirement on reliability in most vehicular applications [46].

In the high-reliability applications where the PER can be greatly reduced and the PRR can be extremely increased, the effective communication range can be highly extended and thus the transmission coverage with the specific PRR requirement can be significantly increased accordingly. Consequently, the large-coverage requirement can be satisfied simultaneously in the ultra-reliable communications.

3.6.3 Transmission Latency and Packet IAT

3.6.3.1 Transmission latency.

The transmission latency, which is also termed as packet duration, is defined as the required time of the PHY to transmit a packet on the wireless medium and can generate a significant influence on the end-to-end latency [31].

3.6.3.1.1 IEEE 802.11p. The transmission latency of IEEE 802.11p can be expressed as [6][31][77]

$$T_{\mathrm{tx}}^{\mathrm{11p}} = T_{\mathrm{pre}}^{\mathrm{11p}} + T_{\mathrm{AIFS}}^{\mathrm{11p}} + T_{\mathrm{sym}}^{\mathrm{11p}} \cdot N_{\mathrm{sym}}^{\mathrm{11p}}, \tag{3.11}$$

where $T_{\mathrm{pre}}^{\mathrm{11p}} = 40\ \mu\mathrm{s}$ is the duration of the Preamble field and the SIGNAL field [9], $T_{\mathrm{AIFS}}^{\mathrm{11p}} = 32\ \mu\mathrm{s}$ is the arbitrary inter-frame space (AIFS) for priority data which is specified as the short inter-frame space (SIFS) for simplicity [46], $T_{\mathrm{sym}}^{\mathrm{11p}} = 8\ \mu\mathrm{s}$ is the duration of an OFDM symbol, and $N_{\mathrm{sym}}^{\mathrm{11p}}$ is the required number of the OFDM symbols obtained by [6]

$$N_{\mathrm{sym}}^{\mathrm{11p}} = \left\lceil \frac{P_{\mathrm{b}} \cdot 8}{N_{\mathrm{sd}}^{\mathrm{11p}} \cdot R^{\mathrm{11p}} \cdot N_{\mathrm{bpsc}}^{\mathrm{11p}}} \right\rceil, \tag{3.12}$$

where P_b is the payload size in bytes which measures the data carried in a packet, $N_{sd}^{11p} = 48$ is the number of data subcarriers in an OFDM symbol, R^{11p} is the coding rate, N_{bpsc}^{11p} is the coded bits per subcarrier, and $\lceil \cdot \rceil$ is a ceiling function applied to round up values to the nearest integer.

The transmission latencies of IEEE 802.11p are compared in Table 3.2 with the 100-byte packet and 1500-byte packet for all MCSs.

3.6.3.1.2 IEEE 802.11bd. The transmission latency of IEEE 802.11bd can be obtained as [6][13]

$$T_{tx}^{11bd} = T_{pre}^{11bd} + T_{AIFS}^{11bd} + T_{sym}^{11bd} \cdot N_{sym}^{11bd} + T_{sym}^{11bd} \cdot N_{ma}, \quad (3.13)$$

where $T_{pre}^{11bd} = 80\ \mu s$ is the duration of the NGV Preamble field, $T_{AIFS}^{11bd} = 32\ \mu s$ is the AIFS for priority data which is simplified as the SIFS, $T_{sym}^{11bd} = 8\ \mu s$ is the OFDM symbol duration, and N_{sym}^{11bd} is the number of the OFDM symbols defined as [6]

$$N_{sym}^{11bd} = \left\lceil \frac{P_b \cdot 8}{N_{sd}^{11bd} \cdot R^{11bd} \cdot N_{bpscs}^{11bd}} \right\rceil, \quad (3.14)$$

where P_b is the packet size in bytes, $N_{sd}^{11bd} = 52$ is the number of data subcarriers in an OFDM symbol, R^{11bd} is the coding rate, N_{bpscs}^{11bd} is the coded bits per subcarrier which equals 0.5 for MCS 15, and $\lceil \cdot \rceil$ is the ceiling function. Moreover, N_{ma} is the number of the OFDM symbols used for midamble which is obtained as [6][11][14]

$$N_{ma} = \left\lfloor \frac{N_{sym}^{11bd} - 1}{T_{ma}} \right\rfloor, \quad (3.15)$$

where T_{ma} is the midamble periodicity which is specified as 4 OFDM symbols for all MCSs to obtain the lowest PER by means of the densest midamble insertion, and $\lfloor \cdot \rfloor$ is a floor function used to round down values to the nearest integer.

The transmission latencies described in IEEE 802.11bd are calculated with the 100-byte and 1500-byte packets respectively which are listed in Table 3.4.

3.6.3.2 Packet IAT.

To measure the time interval between two successive successful packet receptions, the packet IAT is calculated by dividing the packet transmission latency with the PRR, at each given distance for each MCS in an actual communication where the nonzero PER must be considered [31][46].

3.6.4 Theoretical Data Rate, Actual Data Rate, and Effective Data Rate

As the crucial metric to estimate the speed of data transmission in the wireless communications, data rate is known as the number of transmitted data bits per second and measured in bits per second (bps).

3.6.4.1 Theoretical data rate.

The theoretical data rate is calculated as the division between the data bits carried by an OFDM symbol and the OFDM symbol duration [6][9][14]. Since the overhead is not taken into consideration, the theoretical data rate is the ideal maximum data rate but can never be reached in the real communication.

The theoretical data rates of IEEE 802.11p ranging from $3\ \text{Mbps}$ to $27\ \text{Mbps}$ are listed in Table 3.2 for all MCSs [9]. The theoretical data rates of IEEE 802.11bd ranging from $1.625\ \text{Mbps}$ to $39\ \text{Mbps}$ can be achieved as shown in Table 3.4 [14].

3.6.4.2 Actual data rate.

In addition to the data transmission, the transmitted PHY frame for both IEEE 802.11p and IEEE 802.11bd also contains a preamble in each packet and at least one inter-frame space (IFS) between two consecutive packet transmissions [6]. Moreover, there are one or more midambles included in each packet exclusively for the transmitted PHY frame of IEEE 802.11bd. Therefore, the actual data rate is calculated by dividing the data bits transmitted by a packet with the packet duration and is the maximum effective data rate which can be realized in real communication when all the transmitted packets are successfully received. The inevitable overhead in the actual communication gives rise to the actual data rate which is always lower than the theoretical data rate.

3.6.4.2.1 IEEE 802.11p. The actual data rate of IEEE 802.11p can be obtained by means of the payload size P_{b} and transmission latency $T_{\mathrm{tx}}^{\mathrm{11p}}$ with [6][31]

$$\Gamma^{\mathrm{11p}} = \frac{P_{\mathrm{b}} \cdot 8}{T_{\mathrm{tx}}^{\mathrm{11p}}}. \tag{3.16}$$

The actual data rates of IEEE 802.11p are supplied in Table 3.2 with the 100-byte packet and 1500-byte packet for all MCSs.

3.6.4.2.2 IEEE 802.11bd. The actual data rate of IEEE 802.11bd is calculated in terms of the payload P_{b} and transmission latency $T_{\mathrm{tx}}^{\mathrm{11bd}}$ as [6][13]

$$\Gamma^{\mathrm{11bd}} = \frac{P_{\mathrm{b}} \cdot 8}{T_{\mathrm{tx}}^{\mathrm{11bd}}}. \tag{3.17}$$

The actual data rates provided in IEEE 802.11bd are computed with the 100-byte and 1500-byte packets respectively and presented in Table 3.4.

The fixed overhead occupied in the packet results in the difference between the actual data rate and the theoretical data rate, and their gap is dominated by the variable payload size [6][31][46]. With a very large packet size, the packet duration is much larger than the overhead and hence leads to an actual data rate which approaches the theoretical data rate [6]. However, the overhead can bring a significant impact on the applications with very small packet size which generates an obvious decline of the actual data rate from the theoretical data rate [6][31].

3.6.4.3 Effective data rate.

In a practical communication link where the PER is nonzero generally, the effective data rate is obtained by the multiplication of the actual data rate and the PRR for each MCS, at each given distance [46].

CHAPTER FOUR

SIMULATION AND RESULTS

According to the simulation on a complete MATLAB-based PHY modeling [78][79], the PHY performance of both IEEE 802.11p and IEEE 802.11bd are evaluated based on different parameters by means of various metrics for the V2V communications. The framework of the implementation on the simulation whose parameters are summarized in Table 4.1 is displayed in Fig. 4.1.

Table 4.1 Simulation parameters

Parameter	IEEE 802.11p/bd
Transmit Power	23 dBm
Tx Antenna Gain	3 dB
Rx Antenna Gain	3 dB
Reference Path Loss	47.86 dB (at 1 m)
Path-loss Exponent	2.75
Noise Power	-104 dBm
Noise Figure	9 dB
Packet Size	100 bytes (URLLC) 1500 bytes (eMBB)
V2V Channel Model	Urban NLOS Highway NLOS
Channel Bandwidth	10 MHz
Carrier Frequency	5.9 GHz

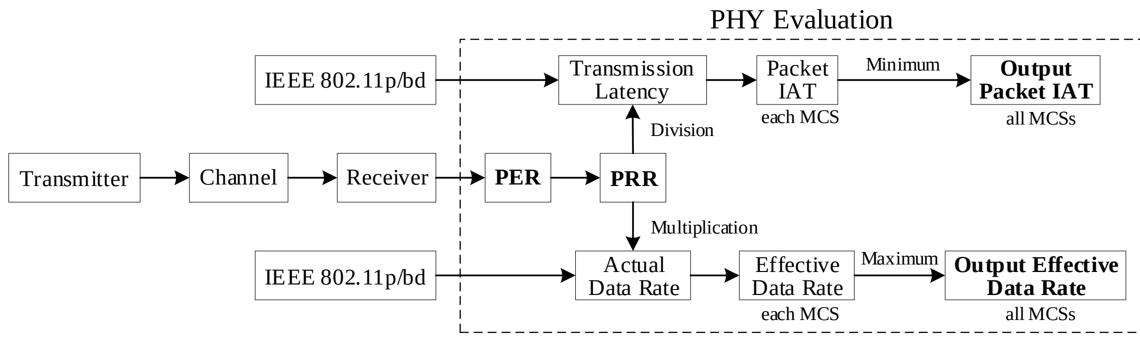

Figure 4.1 Simulation framework

The path loss is defined in the log-distance path-loss model as [24][31]

$$\mathrm{PL}(d) = \mathrm{PL}(d_0) + 10\alpha \log_{10}(d), \tag{4.1}$$

where d is the distance in meters between the transmitter and receiver, α is the path-loss exponent, and $\mathrm{PL}(d_0)$ is the reference path loss at $d_0 = 1$ m obtained as [80]

$$\begin{aligned} \mathrm{PL}(d_0) &= 10\log_{10}\left(\frac{4\pi}{\lambda}\right)^2 d_0^{\alpha} = 10\log_{10}\left(\frac{4\pi}{\lambda}\right)^2 \\ &= 10\log_{10}\left(\frac{4\pi}{c/f_{\mathrm{c}}}\right)^2 = 47.86 \text{ dB}, \end{aligned} \tag{4.2}$$

where λ is the wavelength, $c = 3\times10^8$ m/s is the speed of light, and $f_{\mathrm{c}} = 5.9$ GHz is the carrier frequency.

4.1 IEEE 802.11p

4.1.1 PER

The simulation results of the PER for IEEE 802.11p are displayed with the 100-byte and 1500-byte packets under the urban NLOS scenario in Fig. 4.2 (a) and Fig. 4.2 (b) and under the highway NLOS scenario in Fig. 4.2 (c) and Fig. 4.2 (d), respectively.

For clarity and simplicity, only MCS 2 and MCS 6 are presented in the figures.

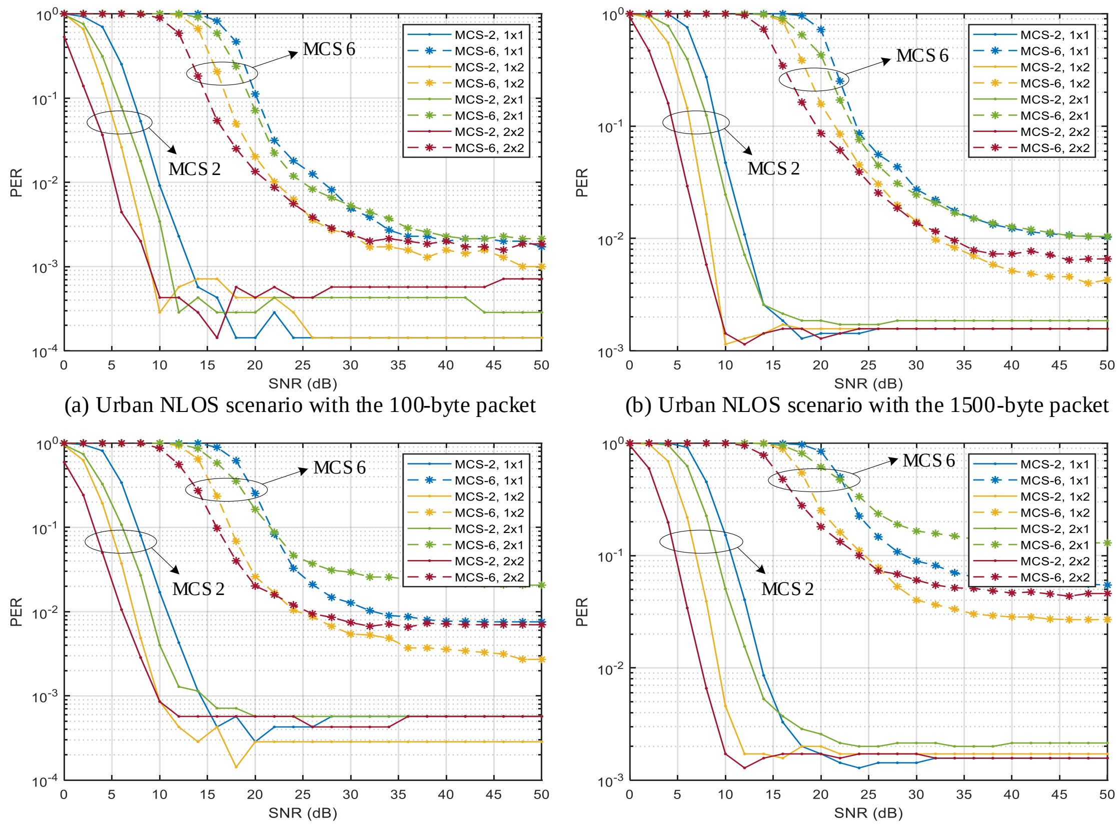

(a) Urban NLOS scenario with the 100-byte packet
(b) Urban NLOS scenario with the 1500-byte packet
(c) Highway NLOS scenario with the 100-byte packet
(d) Highway NLOS scenario with the 1500-byte packet

Figure 4.2 PER in urban NLOS and highway NLOS scenarios with the 100-byte and 1500-byte packets for IEEE 802.11p

4.1.1.1 Impact of antenna configuration.

4.1.1.1.1 SISO. Due to a single transmit antenna and a single receive antenna, the worst performance is revealed with the highest PER in the SISO (1×1) system resulting from the absence of any diversity.

With both packet sizes, both MCSs, and both scenarios, the PER initially experiences the monotonic decrease with the increase of the SNR and finally achieves saturation at the high-SNR range in the SISO system.

4.1.1.1.2 MISO. When there are multiple antennas arranged in the transmitter, the transmit diversity can be realized by the MISO (2×1) system whose PER can be lowered accordingly in comparison with the SISO system.

The PER maintains the monotonic decline for the ascending SNR within the low-SNR range that is followed by the saturation obtained at the higher SNR for all the investigated situations in the MISO system.

4.1.1.1.3 SIMO. If the receiver is configured with multiple antennas, the PER in the SIMO (1×2) system whose receive diversity has been leveraged becomes further lower than that in the MISO and SISO systems.

For both packet sizes with both MCSs in both scenarios, the PER starts from the monotonic drop with the growth of the SNR and falls into saturation eventually in the SIMO system.

Although there are equal multiple antennas at the transmitter in the MISO system and at the receiver in the SIMO system, the SIMO system is still better than the MISO system whose channel state information (CSI) is unknown at the transmitter which leads to a higher PER [53][81].

4.1.1.1.4 MIMO. Once multiple antennas are deployed at the transmitter and receiver, both the transmit diversity and receive diversity are developed and thus the MIMO (2×2) system performs best relying on its lowest PER.

The PER for the MIMO system keeps descending monotonically with the increasing SNR until the emergence of saturation under all the observed conditions.

When the receiver and transmitter are far away from each other, the multi-antenna systems embody their benefits at the lower SNR to exploit the multipath components. Accordingly, in a low-SNR range which is defined below a specific SNR threshold shown in Table 4.2, the MIMO system is the best, the SIMO system is the better, the MISO system is the worse, and the SISO system is the worst regarding the reliability performance.

Table 4.2 SNR thresholds (dB) for PER with IEEE 802.11p

V2V Scenario	100 bytes		1500 bytes	
	MCS 2	MCS 6	MCS 2	MCS 6
Urban NLOS	9.2	25.2	9.6	30.3
Highway NLOS	10	21.8	15	22.3

However, while the receiver gets closer to the transmitter, the interference among multiple antennas becomes predominant at the higher SNR and accordingly the saturated PER in the MIMO, SIMO, or MISO system may be higher than that in the SISO system which breaks the fixed relationship of all the systems within the low-SNR range.

4.1.1.2 Impact of packet size.

4.1.1.2.1 100-byte packet. Beginning at the monotonic decrease with the increase of the SNR and ending at the saturation, the 100-byte packet basically brings the lower

PER and thus fulfills a higher reliability requirement in contrast with the 1500-byte packet. In addition, the smaller packet is less susceptible to the higher MCS and higher Doppler effect. Consequently, the smaller packet is preferred in the high-reliability communications, e.g., URLLC applications.

Furthermore, the SNR threshold with the 100-byte packet is always lower than that with the 1500-byte packet, which discloses that the multi-antenna systems are superior within a smaller low-SNR range for the smaller packet.

4.1.1.2.2 1500-byte packet. By means of the initial monotonic decline with the ascending SNR and the final saturation, the PER is increased and hence the reliability is lower than that with the 100-byte packet.

Moreover, the more severe deterioration emerges for the higher MCS and higher Doppler effect.

4.1.1.3 Impact of MCS.

4.1.1.3.1 MCS 2. During the initial monotonic fall and the following saturation with the increasing SNR, the lower PER is generally caused by MCS 2 and thus the reliability is enhanced accordingly. Moreover, the lower MCS is more resilient to the larger packet and higher Doppler effect. Therefore, the lower MCS is recommended in the ultra-reliable applications.

Besides, the SNR threshold for MCS 2 is greatly reduced and the low-SNR range where the multi-antenna systems are beneficial is shortened significantly.

4.1.1.3.2 MCS 6. According to the beginning monotonic reduction which is followed by the eventual saturation with the growth of the SNR, the PER is elevated and hence the reliability is lowered for MCS 6.

Furthermore, the degradation gets worse for the larger packet and higher Doppler effect.

4.1.1.4 Impact of V2V scenario.

4.1.1.4.1 Urban NLOS scenario. Under the urban scenario with a lower Doppler effect, the PER undergoes the monotonic decline with the rise of the SNR at the lower SNR and enters the saturation at the higher SNR.

Moreover, the urban NLOS scenario usually possesses the slightly lower PER and is more tolerant to the larger packet and higher MCS compared to the highway NLOS scenario.

Additionally, the SNR threshold below which the PER of all the systems can be separated is lower for MCS 2 and higher for MCS 6 than that in the highway NLOS scenario. Therefore, the multi-antenna systems are favorable within a smaller low-SNR range for MCS 2 and within a larger low-SNR range for MCS 6.

4.1.1.4.2 Highway NLOS scenario. With the faster vehicles which result in a higher Doppler effect, the PER in the highway scenario remains the monotonic reduction with the growing SNR before the saturation.

Nevertheless, its PER is often a little higher and the larger packet as well as higher MCS are less endurable compared with the urban NLOS scenario.

The impact of all the parameters, including the antenna configuration, packet size, MCS, and V2V scenario, on the PER for IEEE 802.11p are summarized in Table 4.3 with the applicable range indicated.

Table 4.3 Impact of parameters on PER for IEEE 802.11p

Parameter	PER
Antenna Configuration	MIMO<SIMO<MISO<SISO (Below SNR threshold)
Packet Size	100 bytes<1500 bytes (Mostly)
MCS	MCS 2<MCS 6 (Mostly)
V2V Scenario	Urban NLOS<Highway NLOS (Mostly)

4.1.2 PRR

The simulation results of the PRR for IEEE 802.11p are exhibited with the 100-byte and 1500-byte packets under the urban NLOS scenario in Fig. 4.3 (a) and Fig. 4.3 (b) and under the highway NLOS scenario in Fig. 4.3 (c) and Fig. 4.3 (d) respectively where there are merely MCS 2 and MCS 6 shown for convenience. Several areas have been enlarged to demonstrate the crucial details.

4.1.2.1 Impact of antenna configuration.

4.1.2.1.1 SISO. Without the exploitation of any diversity, the lowest PRR and smallest transmission coverage are uncovered in the SISO (1×1) system which is the least beneficial.

Moreover, the PRR always undergoes the monotonic rise with the decline of the distance and becomes stable at the short-distance range in the SISO system.

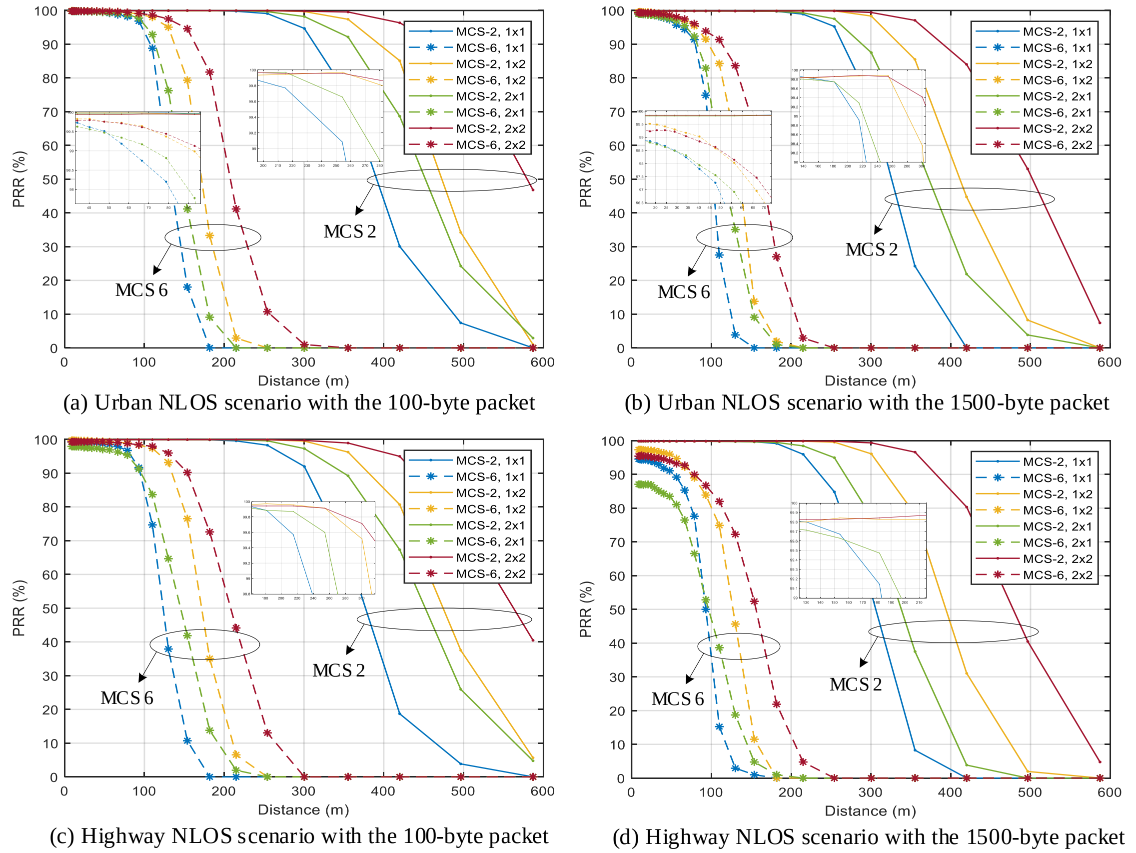

(a) Urban NLOS scenario with the 100-byte packet

(b) Urban NLOS scenario with the 1500-byte packet

(c) Highway NLOS scenario with the 100-byte packet

(d) Highway NLOS scenario with the 1500-byte packet

Figure 4.3 PRR in urban NLOS and highway NLOS scenarios with the 100-byte and 1500-byte packets for IEEE 802.11p

4.1.2.1.2 MISO. Relying on the higher PRR and larger coverage, the MISO (2×1) system is superior to the SISO system.

Besides, the monotonic increase of the PRR with the descending distance is terminated with the stability for the shorter distance in the MISO system.

4.1.2.1.3 SIMO. Since the PRR and coverage are further improved, the SIMO (1×2) system is preferable to the MISO and SISO systems.

Additionally, the PRR for the SIMO system is monotonically ascending with the reduction of the distance until its encounter with the stability at the shorter distance.

4.1.2.1.4 MIMO. Based on the most sufficient utilization of diversity, the MIMO (2×2) system is the most favorable with the highest PRR and largest coverage.

Furthermore, the monotonic growth of the PRR with the decreasing distance is continued with the stability ultimately in the MIMO system.

To completely and consistently evaluate the coverage with the specific packet size, MCS, and Doppler effect in various antenna configurations, the basic coverage, which can be guaranteed by all the antenna configurations, is defined as the minimum coverage in the MIMO, SIMO, MISO, and SISO systems. Specifically, the basic coverages which can meet the requirement on 90% PRR for the given packet and MCS configurations under both NLOS scenarios are listed in Table 4.4.

Table 4.4 Basic coverages (m) with 90% PRR requirement for IEEE 802.11p

V2V Scenario	100 bytes		1500 bytes	
	MCS 2	MCS 6	MCS 2	MCS 6
Urban NLOS	313	108	265	80
Highway NLOS	305	95	236	N/A

Corresponding to the PER of MCS 6 for the 2×1 system which is always higher than 10^{-1} with the 1500-byte packet under the highway NLOS scenario, the resulting PRR is always lower than 90% and the basic coverage for the 90% PRR requirement does not exist due to the lack of generality.

Different from the short-distance range where the multi-antenna interference is dominant and may lead to the lower PRR and smaller coverage in the MIMO, SIMO, or MISO system than that in the SISO system, the multi-antenna systems become favorable in utilizing the multipath at the farther distance. Consequently, the PRR and coverage performances are the best, better, worse, and worst with the MIMO, SIMO, MISO, and SISO systems respectively within the far-distance range above a specific distance threshold listed in Table 4.5.

Table 4.5 Distance thresholds (m) for PRR with IEEE 802.11p

V2V Scenario	100 bytes		1500 bytes	
	MCS 2	MCS 6	MCS 2	MCS 6
Urban NLOS	259	70	255	46
Highway NLOS	254	94	168	90

4.1.2.2 Impact of packet size.

4.1.2.2.1 100-byte packet. The PRR with the 100-byte packet initiates the monotonic rise with the reduction of the distance which is proceeded with stability.

Usually, the higher PRR and larger coverage can be reached which lead to the expansion of the basic coverage. Hence, its basic coverage is always larger than that with the 1500-byte packet under all the investigated conditions. Besides, the smaller packet is more resistant to the higher MCS and higher Doppler effect. Accordingly, the basic coverage is still valid for 95 m although MCS 6 and the highway NLOS scenario are adopted.

Furthermore, the higher distance threshold for the 100-byte packet narrows the far-distance range where the multi-antenna systems are beneficial.

4.1.2.2.2 1500-byte packet. During the monotonic growth and the succeeding stability with the descending distance, the PRR is reduced and hence the coverage is diminished for the 1500-byte packet.

More affected by the higher MCS and higher Doppler effect, the basic coverage for MCS 6 under the highway NLOS scenario is disabled.

4.1.2.3 Impact of MCS.

4.1.2.3.1 MCS 2. The PRR of MCS 2 begins with the monotonic increase and terminates with the stability along with the reducing distance.

The PRR is often elevated, hence, the coverage is enlarged which gives rise to the larger basic coverage. Accordingly, its basic coverage is significantly greater than that for MCS 6. Less vulnerable to the larger packet and higher Doppler effect, the basic coverage of 236 m can still be realized even if the 1500-byte packet and highway NLOS scenario are encountered.

Moreover, the distance threshold is extremely higher for MCS 2 which remarkably limits the far-distance range where the multi-antenna systems are favorable.

4.1.2.3.2 MCS 6. Based on the initial monotonic growth and the final stability with the decrease in distance, the PRR gets lower and hence the coverage becomes smaller compared to that with MCS 2.

More influenced by the larger packet and higher Doppler effect, the basic coverage is invalid in the highway NLOS scenario with the 1500-byte packet.

4.1.2.4 Impact of V2V scenario.

4.1.2.4.1 Urban NLOS scenario. The PRR in the urban NLOS scenario initially experiences the monotonic increase and then remains stable with the decline of the distance.

Generally, the PRR is slightly higher and hence the coverage is somewhat extended. As a result, the basic coverage is also extended with the simultaneous expansion of the coverage in all antenna configurations. Consequently, its basic coverage is always larger than that in the highway NLOS scenario for all the observed situations. Moreover, the urban NLOS scenario is less sensitive to the larger packet and higher MCS. Thus, the basic coverage can still reach as far as 80 m even for MCS 6 with the 1500-byte packet.

The distance threshold of the PRR is higher for MCS 2 and lower for MCS 6 in contrast with the highway NLOS scenario. Accordingly, the multi-antenna systems are conducive within a smaller far-distance range for MCS 2 and within a larger far-distance range for MCS 6.

4.1.2.4.2 Highway NLOS scenario. Experiencing the monotonic growth and the subsequent stability with the decreasing distance, the PRR is lowered and thus the coverage is shortened in the highway NLOS scenario.

Less tolerable to the larger packet and higher MCS, the basic coverage for MCS 6 with the 1500-byte packet cannot be realized.

The impact of all the parameters, including the antenna configuration, packet size, MCS, and V2V scenario, on the PRR for IEEE 802.11p are summarized in Table 4.6 with the applicable range indicated.

Table 4.6 Impact of parameters on PRR for IEEE 802.11p

Parameter	PRR
Antenna Configuration	MIMO>SIMO>MISO>SISO (Above distance threshold)
Packet Size	100 bytes>1500 bytes (Mostly)
MCS	MCS 2>MCS 6 (Mostly)
V2V Scenario	Urban NLOS>Highway NLOS (Mostly)

4.1.3 Output Packet IAT

Due to the variation on distance between the receiver and transmitter which results in the changing SNRs with different channel fading conditions, the output packet IAT, which is defined as the minimum packet IAT for all MCSs, can be obtained in the link adaptation at each observed distance which can better accommodate the channel characteristics [46].

The simulation results of the output packet IAT for IEEE 802.11p with the 100-byte and 1500-byte packets are illustrated under the urban NLOS scenario in Fig. 4.4 (a) and Fig. 4.4 (b) and under the highway NLOS scenario in Fig. 4.4 (c) and Fig. 4.4 (d), respectively. Certain areas have been amplified to exhibit the necessary details.

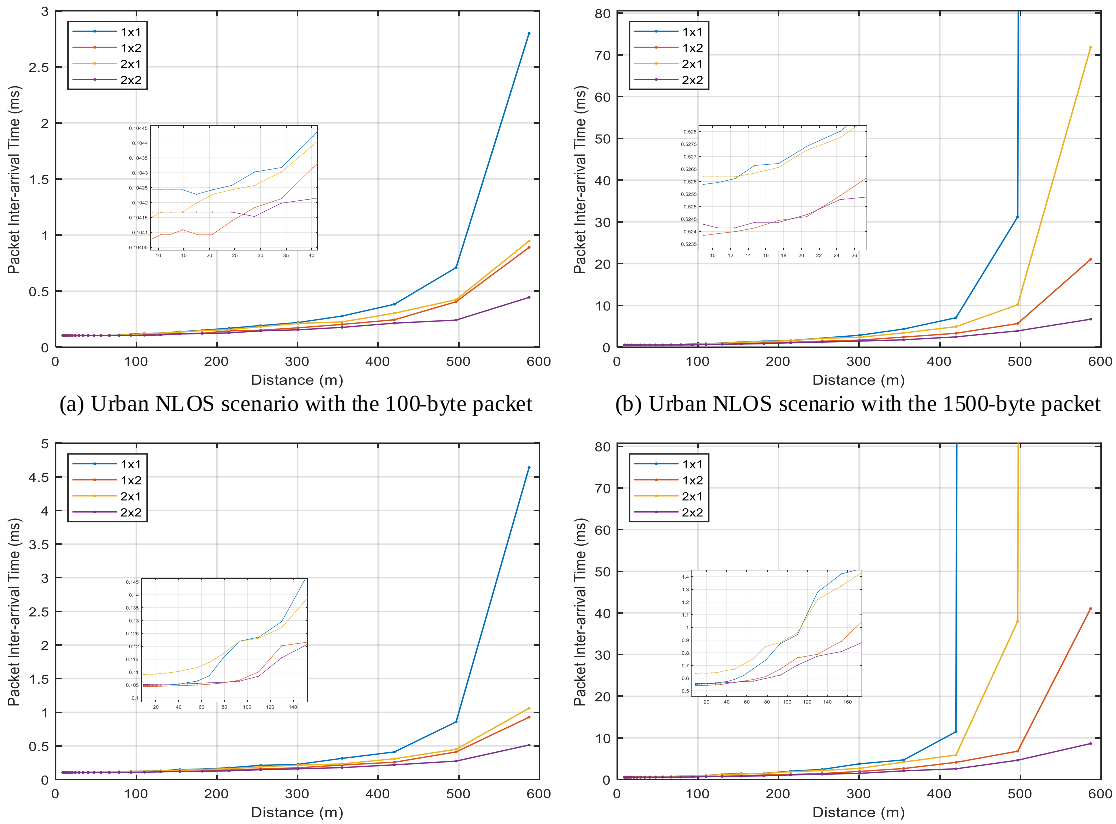

(a) Urban NLOS scenario with the 100-byte packet

(b) Urban NLOS scenario with the 1500-byte packet

(c) Highway NLOS scenario with the 100-byte packet

(d) Highway NLOS scenario with the 1500-byte packet

Figure 4.4 Output packet IAT in urban NLOS and highway NLOS scenarios with the 100-byte and 1500-byte packets for IEEE 802.11p

4.1.3.1 Impact of antenna configuration.

4.1.3.1.1 SISO. The output packet IAT is monotonically decreasing with the reduction of the distance in the SISO (1×1) system and remains largest in all the antenna configurations above the distance threshold.

Most vulnerable to the larger packet, the packet IAT with the 1500-byte packet suffers from the abrupt growth with the increasing distance not only under the highway NLOS scenario but also under the urban NLOS scenario, and both the resulting packet IATs approach infinity at the farther distance.

4.1.3.1.2 MISO. Based on the monotonic decline with the descending distance, the output packet IAT is decreased in the MISO (2×1) system than that in the SISO system above the distance threshold.

More sensitive to the larger packet and higher Doppler effect, the packet IAT with the 1500-byte packet under the highway NLOS scenario is close to infinity after the steep increase with the ascending distance at the farther distance.

4.1.3.1.3 SIMO. The output packet IAT follows the monotonic decrease with the diminishing distance in the SIMO (1×2) system and is further reduced in comparison to the SISO and MISO systems above the distance threshold.

4.1.3.1.4 MIMO. According to the monotonic decline with the decrease in distance, the output packet IAT is smallest in the MIMO (2×2) system which outperforms the SIMO, MISO, and SISO systems above the distance threshold.

Contrary to the multi-antenna configurations that may lead to the larger packet IAT in comparison to the single-antenna configuration because of the interference generated at the short distance, the multi-antenna systems become beneficial in applying the multipath components over the longer distance. Accordingly, the MIMO, SIMO, MISO, and SISO systems perform best, better, worse, and worst on the packet IAT respectively in the long-distance range above the distance threshold demonstrated in Table 4.7.

Table 4.7 Distance thresholds (m) for output packet IAT with IEEE 802.11p

V2V Scenario	100 bytes	1500 bytes
Urban NLOS	27	22
Highway NLOS	93	114

4.1.3.2 Impact of packet size.

4.1.3.2.1 100-byte packet. The output packet IAT with the 100-byte packet follows the monotonic decrease with the reduction in distance gradually and is always smaller than that with the 1500-byte packet which is preferable for the low-latency communications. Less susceptible to the higher Doppler effect, the degeneration on the packet IAT in the highway NLOS scenario is effectively suppressed and the infinite packet IAT at the farther distance can be avoided for both scenarios.

The distance threshold with the 100-byte packet which is lower in the highway NLOS scenario and higher in the urban NLOS scenario compared to the 1500-byte packet respectively expands and shortens the far-distance range where the multi-antenna systems are favorable.

4.1.3.2.2 1500-byte packet. After the steep and monotonic growth of the packet IAT with the increasing distance, the resulting packet IAT with the 1500-byte packet is extremely higher than that with the 100-byte packet and the infinite packet IAT appears in both the urban NLOS and highway NLOS scenarios over longer distance. Furthermore, the gap between both scenarios is enlarged with the larger packet.

4.1.3.3 Impact of V2V scenario.

4.1.3.3.1 Urban NLOS scenario. The output packet IAT undergoes the monotonic drop with the decreasing distance and is usually smaller compared to the highway NLOS scenario. More tolerant to the larger packet, the advantage of the urban NLOS scenario over the highway NLOS scenario becomes more prominent with the 1500-byte packet.

Additionally, the quite smaller distance threshold greatly extends the far-distance range where the multi-antenna systems are conducive.

4.1.3.3.2 Highway NLOS scenario. During the monotonic decline with the reducing distance, the increase of the packet IAT compared with the urban NLOS scenario is more remarkable with the 1500-byte packet. Accordingly, the infinite packet IAT at the farther distance occurs in both the 1×1 and 2×1 systems after the more dramatic rise with the increase of the distance for the highway NLOS scenario but exclusively in the 1×1 system for the urban NLOS scenario.

The impact of all the parameters, including the antenna configuration, packet size, and V2V scenario, on the output packet IAT for IEEE 802.11p are summarized in Table 4.8 with the applicable range indicated.

Table 4.8 Impact of parameters on output packet IAT for IEEE 802.11p

Parameter	Output Packet IAT
Antenna Configuration	MIMO < SIMO < MISO < SISO (Above distance threshold)
Packet Size	100 bytes < 1500 bytes (Always)
V2V Scenario	Urban NLOS < Highway NLOS (Mostly)

4.1.4 Output Effective Data Rate

Since the SNR is varying with the changing distances and channel fading conditions, the output effective data rate, defined as the maximum effective data rate for all MCSs, can be caught by the link adaptation at each specified distance [31][46].

The simulation results of the output effective data rate for IEEE 802.11p with the 100-byte and 1500-byte packets are demonstrated under the urban NLOS scenario in Fig. 4.5 (a) and Fig. 4.5 (b) and under the highway NLOS scenario in Fig. 4.5 (c) and Fig. 4.5 (d), respectively. Some areas have been zoomed in to show the essential details.

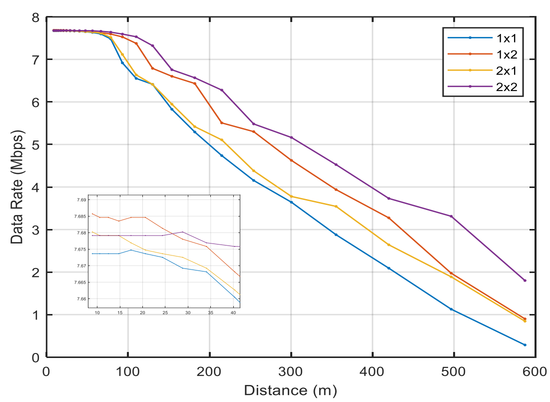

(a) Urban NLOS scenario with the 100-byte packet

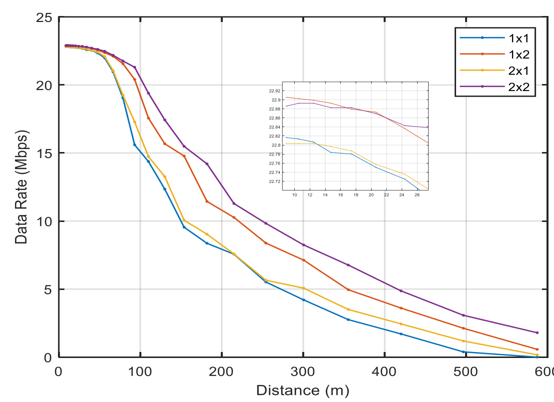

(b) Urban NLOS scenario with the 1500-byte packet

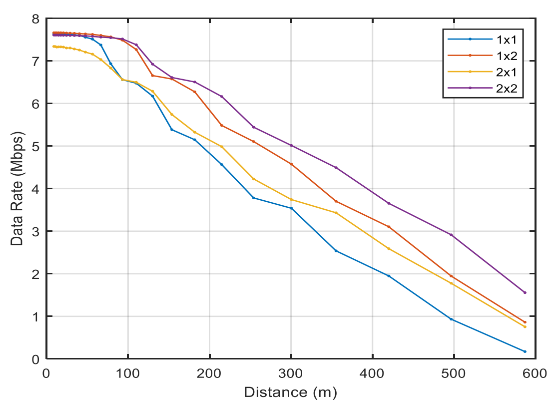

(c) Highway NLOS scenario with the 100-byte packet

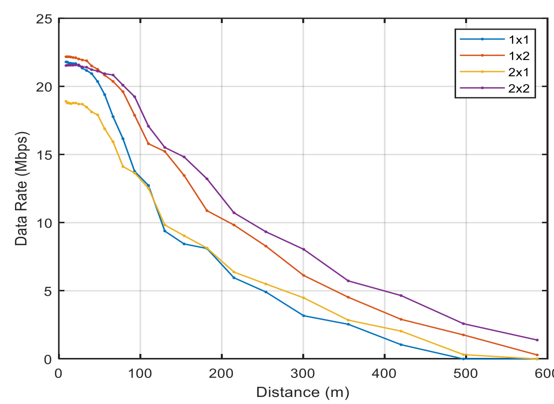

(d) Highway NLOS scenario with the 1500-byte packet

Figure 4.5 Output effective data rate in urban NLOS and highway NLOS scenarios with the 100-byte and 1500-byte packets for IEEE 802.11p

4.1.4.1 Impact of antenna configuration.

4.1.4.1.1 SISO. The output effective data rate undergoes the monotonic growth with the decline in distance under all the observed situations in the SISO (1×1) system and is lowest in all the antenna configurations above a specific distance threshold.

4.1.4.1.2 MISO. According to the monotonic rise with the reducing distance, the output effective data rate is improved in the MISO (2×1) system compared with the SISO system above the distance threshold.

4.1.4.1.3 SIMO. During the monotonic increase with the decrease in distance, the output effective data rate can be further enhanced above the distance threshold in the SIMO (1×2) system compared with the MISO and SISO systems.

4.1.4.1.4 MIMO. The output effective data rate experiences the monotonic growth with the diminishing distance in the MIMO (2×2) system and surpasses that from all the other systems above the distance threshold.

Instead of the interference which occurs within the short distance and sometimes generates the lower data rate in the multi-antenna configurations in comparison to the single-antenna configuration, the multipath components can be exerted in the multi-antenna architectures over the longer distance. Consequently, the best, better, worse, and worst performances on the data rate are exhibited in the MIMO, SIMO, MISO, and SISO systems respectively at the far-distance range above the distance threshold illustrated in Table 4.9.

Table 4.9 Distance thresholds (m) for output effective data rate with IEEE 802.11p

V2V Scenario	100 bytes	1500 bytes
Urban NLOS	27	22
Highway NLOS	93	116

4.1.4.2 Impact of packet size.

4.1.4.2.1 100-byte packet. The output effective data rate with the 100-byte packet, which is often lower than that with the 1500-byte packet, experiences the monotonic growth with the decreasing distance gently. More resilient to the higher Doppler effect, the gap can be constrained significantly between the highway NLOS scenario and urban NLOS scenario.

The distance threshold with the 100-byte packet that is lower for the highway NLOS scenario and higher for the urban NLOS scenario compared to the 1500-byte packet respectively represents the larger and smaller far-distance range where the multi-antenna systems are beneficial.

4.1.4.2.2 1500-byte packet. Due to the sharp increase, which is monotonic, with the decline in distance, the higher data rate can still be obtained with the 1500-byte packet for the majority in distance even though the minimum data rate over the farthest distance is close to that with the 100-byte packet. Thus, the larger packet maintains its superiority in the high-throughput applications.

Besides, the degradation on the data rate with the higher Doppler effect becomes worse with the larger packet and the extraordinary distinction exists at the short distance within 100 m between both scenarios.

4.1.4.3 Impact of V2V scenario.

4.1.4.3.1 Urban NLOS scenario. The output effective data rate always follows the monotonic rise with the reduction in distance for the urban NLOS scenario and is generally higher than that for the highway NLOS scenario. With more superiority than the highway NLOS scenario for the larger packet, the urban NLOS scenario is more resistant to the challenging larger packet.

In addition, the distance threshold is much smaller and hence the multi-antenna systems are beneficial within an extremely longer far-distance range.

4.1.4.3.2 Highway NLOS scenario. Based on the monotonic increase with the descending distance, the deterioration in the output effective data rate under the highway NLOS scenario emerges and becomes more serious with the larger packet. Specifically, compared to the urban NLOS scenario whose initial data rates with the 1500-byte packet are always higher than $22\ \text{Mbps}$, the initial data rates with the 1500-byte packet under the highway NLOS scenario drop slightly in the 1×1 and 2×2 systems which are merely below $22\ \text{Mbps}$ and seriously in the 2×1 system which is even below $19\ \text{Mbps}$.

The impact of all the parameters, including the antenna configuration, packet size, and V2V scenario, on the output effective data rate for IEEE 802.11p are summarized in Table 4.10 with the applicable range indicated.

4.2 IEEE 802.11bd

4.2.1 PER

The simulation results of the PER for IEEE 802.11bd are shown with the 100-byte and 1500-byte packets under the urban NLOS scenario in Fig. 4.6 (a) and Fig. 4.6 (b) and under the highway NLOS scenario in Fig. 4.6 (c) and Fig. 4.6 (d), respectively.

Since MCS 1 and MCS 5 of IEEE 802.11bd are respectively corresponding to MCS 2 and MCS 6 of IEEE 802.11p which are selected in the previous exhibition, there are merely MCS 1 and MCS 5 shown in IEEE 802.11bd not only for clarity and simplicity but also for the direct comparison with IEEE 802.11p.

Table 4.10 Impact of parameters on output effective data rate for IEEE 802.11p

Parameter	Output Effective Data Rate
Antenna Configuration	MIMO>SIMO>MISO>SISO (Above distance threshold)
Packet Size	1500 bytes>100 bytes (Mostly)
V2V Scenario	Urban NLOS>Highway NLOS (Mostly)

4.2.1.1 Impact of antenna configuration.

4.2.1.1.1 SISO. Since there is only one antenna at the transmitter and one antenna at the receiver, the SISO (1×1) system performs worst with the highest PER due to the lack of transmit diversity and receive diversity.

Moreover, the PER of the SISO system always decreases monotonically with the increase of the SNR initially and reaches saturation finally, which is applicable for both packet sizes, both MCSs, and both scenarios.

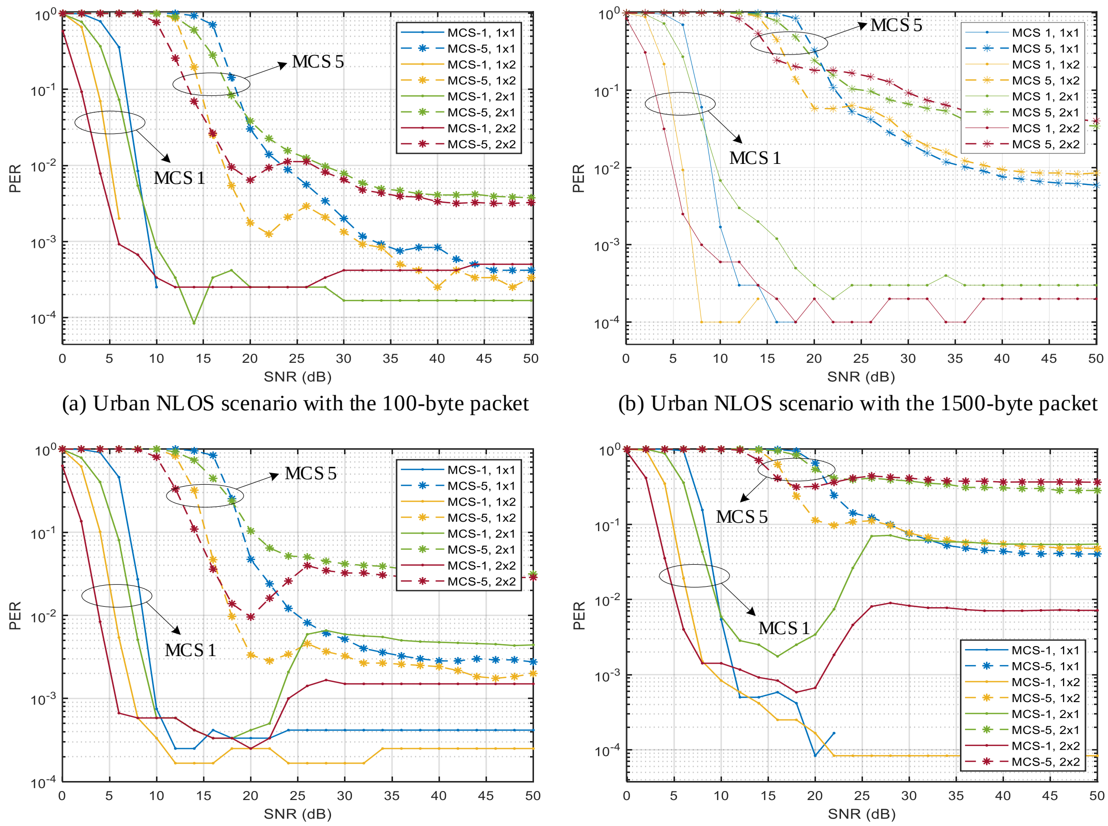

(a) Urban NLOS scenario with the 100-byte packet

(b) Urban NLOS scenario with the 1500-byte packet

(c) Highway NLOS scenario with the 100-byte packet

(d) Highway NLOS scenario with the 1500-byte packet

Figure 4.6 PER in urban NLOS and highway NLOS scenarios with the 100-byte and 1500-byte packets for IEEE 802.11bd

4.2.1.1.2 MISO. With multiple transmit antennas and a single receive antenna, the transmit diversity is developed in the MISO (2×1) system and thus the PER is reduced compared to the SISO system.

Due to the absence of the CSI at the transmitter, the performance of the MISO system is inferior to the SIMO system because of its higher PER even if the number of transmit antennas in the MISO system is equal to the number of receive antennas in the SIMO system.

The occasional growth of the PER with the increase of the SNR emerges in the highway NLOS scenario with the 100-byte packet for MCS 1 and with the 1500-byte packet for both MCSs.

4.2.1.1.3 SIMO. Because of the advantage of the receive diversity, the SIMO (1×2) system, with multiple receive antennas and a single transmit antenna, is superior to both the MISO and SISO systems in terms of the further reduced PER.

The undesired rise of the PER with the increase of the SNR occurs in both scenarios with both packet sizes for MCS 5.

4.2.1.1.4 MIMO. Based on the full employment of both transmit diversity and receive diversity obtained by multiple transmit antennas and multiple receive antennas, the MIMO (2×2) system is optimal with the lowest PER among all the antenna configurations.

The abnormal increase of the PER with the increase of the SNR exists in the urban NLOS scenario with the 100-byte packet for MCS 5 and in the highway NLOS scenario with both packet sizes for both MCSs.

When the transmitter is far away from the receiver which results in the low SNR, the multi-antenna configurations are advantageous in utilizing the multipath components. Consequently, below a specific SNR threshold which corresponds to a low-SNR range and thus a long-distance range, the SISO system is inferior to the multi-antenna systems in which the MIMO system is the best, the SIMO system is the better, and the MISO system is the worst. Specifically, the SNR thresholds of the PER respectively for MCS 1 and MCS 5 with the 100-byte and 1500-byte packets under the urban NLOS and highway NLOS scenarios are listed in Table 4.11.

Table 4.11 SNR thresholds (dB) for PER with IEEE 802.11bd

V2V Scenario	100 bytes		1500 bytes	
	MCS 1	MCS 5	MCS 1	MCS 5
Urban NLOS	6	15.9	6.7	17.2
Highway NLOS	8	16.9	8.2	17.2

However, with the smaller distance between the transmitter and receiver and thus the higher SNR, the multi-antenna interference becomes dominant. Hence, the abnormal increase of the PER with the increase of the SNR is not found in the SISO system but widely present under the MISO, SIMO, and MIMO systems instead. Furthermore, the saturated PER in certain multi-antenna systems, MISO, SIMO, or MIMO, can exceed that in the SISO system as the result of multi-antenna interference. The earliest minimum PER during the increase of the SNR, the second maximum PER, and the ratio between them, which are combined to measure the temporary growth of the PER, are shown in Table 4.12. The saturated PER at the highest SNR and its relative value compared to the earliest minimum PER are also provided as reference. In addition, the SNR at which the earliest minimum PER, the second maximum PER, and the saturated PER appear are given as well.

4.2.1.2 Impact of packet size.

4.2.1.2.1 100-byte packet. The 100-byte packet mainly generates the smaller PER compared to the 1500-byte packet even if an occasional rise of the PER is present, which is helpful to maintain a lower PER level and satisfy a higher reliability requirement.

Moreover, the smaller packet is less influenced by the higher MCS and higher Doppler effect. Hence, the smaller packet is recommended in the ultra-reliable communication, e.g., URLLC application.

Instead of the monotonic reduction with the increase of the SNR, the temporary growth of the PER occurs for MCS 5 in the 1×2 and 2×2 systems in both scenarios and for MCS 1 in the 2×1 and 2×2 systems in the highway NLOS scenario.

Table 4.12 Abnormal increase of PER with increase of SNR for IEEE 802.11bd

V2V Scenario	Packet Size (bytes)	MCS	Antenna Setup	Earliest Minimum PER (SNR)	Second Maximum PER (SNR)	Relative PER	Saturated PER (SNR)	Relative PER
Urban NLOS	100	5	SIMO	0.00125 (22 dB)	0.00292 (26 dB)	2.34	0.00033 (50 dB)	0.26
Urban NLOS	100	5	MIMO	0.00642 (20 dB)	0.01123 (24 dB)	1.75	0.00325 (50 dB)	0.51
Urban NLOS	1500	5	SIMO	0.0581 (20 dB)	0.0632 (24 dB)	1.09	0.0085 (50 dB)	0.15
Highway NLOS	100	1	MISO	0.00033 (16 dB/ 18 dB)	0.00658 (28 dB)	19.94	0.00442 (50 dB)	13.39
Highway NLOS	100	1	MIMO	0.00025 (20 dB)	0.00167 (28 dB)	6.68	0.0015 (50 dB)	6
Highway NLOS	100	5	SIMO	0.00283 (22 dB)	0.00458 (26 dB)	1.62	0.002 (50 dB)	0.71
Highway NLOS	100	5	MIMO	0.00956 (20 dB)	0.03971 (26 dB)	4.15	0.02853 (50 dB)	2.98
Highway NLOS	1500	1	MISO	0.00175 (16 dB)	0.07138 (28 dB)	40.79	0.05459 (50 dB)	31.19
Highway NLOS	1500	1	MIMO	0.00058 (18 dB)	0.00899 (28 dB)	15.5	0.00717 (50 dB)	12.36
Highway NLOS	1500	5	SIMO	0.0969 (22 dB)	0.11173 (26 dB)	1.15	0.04757 (50 dB)	0.49
Highway NLOS	1500	5	MISO	0.39216 (24 dB)	0.41322 (26 dB)	1.05	0.28169 (50 dB)	0.72
Highway NLOS	1500	5	MIMO	0.31348 (18 dB)	0.44053 (26 dB)	1.41	0.36364 (50 dB)	1.16

Moreover, with the lower SNR threshold, the smaller packet brings a smaller low-SNR range for the multi-antenna systems to demonstrate their predominance.

The PER of MCS 1 can be as low as 0 in the 1×1 and 1×2 systems under the urban NLOS scenario and cannot be shown in the logarithmic-scale figure.

4.2.1.2.2 1500-byte packet. With the higher PER and thus the lower reliability, the degradation on the 1500-byte packet becomes even worse with the higher MCS and higher Doppler effect.

The unusual rise of the PER with the 1500-byte packet is similar to that with the 100-byte packet, except that the 2×2 system for MCS 5 in the urban NLOS scenario is excluded and the 2×1 system for MCS 5 in the highway NLOS scenario is included.

In addition to the 1×1 and 1×2 systems in the urban NLOS scenario, the PER of MCS 1 can also be reduced to 0 in the 1×1 system under the highway NLOS scenario.

4.2.1.3 Impact of MCS.

4.2.1.3.1 MCS 1. MCS 1 often realizes the lower PER and reaches a higher reliability in contrast with MCS 5, even with the existence of the unfavorable rise of the PER. Besides, the lower MCS is less vulnerable to the larger packet size and higher Doppler effect. Thus, the lower MCS is introduced for the more reliable and robust transmission.

Beginning with the monotonic decrease with the increasing SNR, the following PER undergoes the unexpected increase in the 2×1 and 2×2 systems with both packet sizes under the highway NLOS scenario.

In addition, the lower SNR threshold brought by the lower MCS reduces the low-SNR range over which the multi-antenna systems are beneficial.

4.2.1.3.2 MCS 5. With the increased PER which lowers reliability, the inferiority of MCS 5 compared with MCS 1 becomes more obvious for the larger packet size and higher Doppler effect.

The destructive growth of the PER emerges in the 1×2 and 2×2 systems with the 100-byte packet under both scenarios, in the 1×2, 2×1, and 2×2 systems with the 1500-byte packet under the highway NLOS scenario, and in the 1×2 system with the 1500-byte packet under the urban NLOS scenario.

Different from MCS 1 for which the PER can be sometimes decreased to 0, the PER can never be fallen to 0 for MCS 5.

4.2.1.4 Impact of V2V scenario.

4.2.1.4.1 Urban NLOS scenario. In the urban scenario with the slower movement of vehicles, the PER is generally monotonically decreasing with the increase of the SNR until the occurrence of saturation. Exceptionally, there is an undesired rise of the PER exclusively for MCS 5 in the 1×2 and 2×2 systems with the 100-byte packet and in the 1×2 system with the 1500-byte packet.

With the lower PER, the urban NLOS scenario with the lower Doppler effect is less sensitive to the larger packet size and higher MCS.

The SNR threshold below which the PER of various systems can be distinguished is smaller than or equal to that in the highway NLOS scenario for MCS 1 and MCS 5, which indicates that the multi-antenna configurations are beneficial in a smaller or equal low-SNR range and thus a smaller or equal long-distance range.

The PER of MCS 1 is equal to 0 with the 100-byte packet above 10 dB in the 1×1 system and above 6 dB in the 1×2 system respectively, and with the 1500-byte packet above 18 dB in the 1×1 system and above 14 dB in the 1×2 system respectively.

4.2.1.4.2 Highway NLOS scenario. Due to the higher Doppler effect caused by the faster vehicles in the highway scenario, the PER is usually slightly higher than that in the urban NLOS scenario and the larger packet size and higher MCS are less tolerable.

The abnormal increase of the PER is extensively present with both packet sizes for MCS 1 in the 2×1 and 2×2 systems and for MCS 5 in the 1×2 and 2×2 systems, and solely with the 1500-byte packet for MCS 5 in the 2×1 system.

The PER of MCS 1 equals to 0 above 22 dB in the 1×1 system with the 1500-byte packet.

The impact of all the parameters, including the antenna configuration, packet size, MCS, and V2V scenario, on the PER for IEEE 802.11bd are concluded in Table 4.13 with the applicable range indicated.

Table 4.13 Impact of parameters on PER for IEEE 802.11bd

Parameter	PER
Antenna Configuration	MIMO<SIMO<MISO<SISO (Below SNR threshold)
Packet Size	100 bytes<1500 bytes (Mostly)
MCS	MCS 1<MCS 5 (Mostly)
V2V Scenario	Urban NLOS<Highway NLOS (Mostly)

4.2.2 PRR

The simulation results of the PRR for IEEE 802.11bd, which involve only MCS 1 and MCS 5, are illustrated with the 100-byte and 1500-byte packets under the urban NLOS scenario in Fig. 4.7 (a) and Fig. 4.7 (b) and under the highway NLOS scenario in Fig. 4.7 (c) and Fig. 4.7 (d), respectively. Certain areas have been magnified to illustrate the important details.

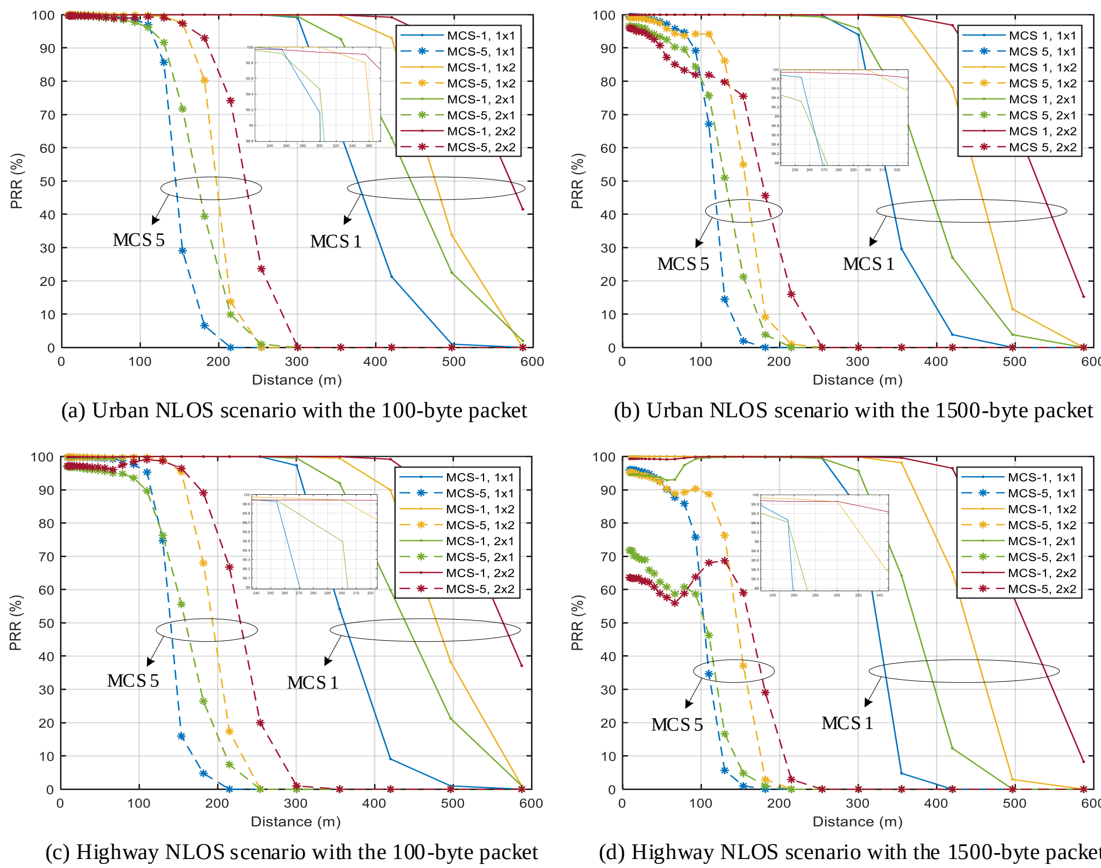

(a) Urban NLOS scenario with the 100-byte packet

(b) Urban NLOS scenario with the 1500-byte packet

(c) Highway NLOS scenario with the 100-byte packet

(d) Highway NLOS scenario with the 1500-byte packet

Figure 4.7 PRR in urban NLOS and highway NLOS scenarios with the 100-byte and 1500-byte packets for IEEE 802.11bd

4.2.2.1 Impact of antenna configuration.

4.2.2.1.1 SISO. Without the adoption of transmit diversity and receive diversity, the SISO (1×1) system is the least favorable with the lowest PRR and the smallest transmission coverage.

Furthermore, the PRR of the SISO system always experiences the monotonic increase with the decrease of distance and then remains stable for both MCSs with both packet sizes in both scenarios.

4.2.2.1.2 MISO. The PRR and coverage can be increased in the MISO (2×1) system which becomes preferable in comparison with the SISO system.

In accordance with the occasional growth of the PER with the increase of the SNR, the incidental reduction of the PRR with the decrease of the distance appears in the highway NLOS scenario for MCS 1 with both packet sizes and for MCS 5 with the 1500-byte packet.

4.2.2.1.3 SIMO. Depending on the further increased PRR and coverage, the SIMO (1×2) system is more beneficial than the MISO and SISO systems.

The unexpected drop of the PRR with the decrease of the distance happens for MCS 5 with both packet sizes under both scenarios.

4.2.2.1.4 MIMO. Due to the highest PRR and the largest coverage, the MIMO (2×2) system is the most advantageous in all the antenna configurations.

The harmful decline of the PRR with the decrease of the distance is present under the urban NLOS scenario for MCS 5 with the 100-byte packet and under the highway NLOS scenario for both MCSs with both packet sizes.

The basic coverages with respect to the 90% PRR requirement for MCS 1 and MCS 5 with the 100-byte and 1500-byte packets in the urban NLOS and highway NLOS scenarios are shown in Table 4.14.

Table 4.14 Basic coverages (m) with 90% PRR requirement for IEEE 802.11bd

V2V Scenario	100 bytes		1500 bytes	
	MCS 1	MCS 5	MCS 1	MCS 5
Urban NLOS	315	122	304	49
Highway NLOS	310	109	283	N/A

Since the PERs of MCS 5 for the 2×1 and 2×2 systems are always above 10^{-1} in the highway NLOS scenario with the 1500-byte packet, the corresponding PRRs are always below 90% and the generality of the basic coverage for the 90% PRR target cannot be satisfied which disables its validity.

Contrary to the multi-antenna systems which may result in the lower PRR and the smaller coverage due to the interference in the short-distance range compared to the SISO system, the multi-antenna configurations are helpful to exploit the multipath in the long-distance range and thus the multi-antenna systems are better than the SISO system with the higher PRR above a specific distance threshold. Specifically, the distance thresholds of the PRR respectively for MCS 1 and MCS 5 with the 100-byte and 1500-byte packets under the urban NLOS and highway NLOS scenarios are illustrated in Table 4.15.

Table 4.15 Distance thresholds (m) for PRR with IEEE 802.11bd

V2V Scenario	100 bytes		1500 bytes	
	MCS 1	MCS 5	MCS 1	MCS 5
Urban NLOS	321	154	307	136
Highway NLOS	300	137	295	136

4.2.2.2 Impact of packet size.

4.2.2.2.1 100-byte packet. Basically, the higher PRR and the larger coverage are obtained by the 100-byte packet in comparison with the 1500-byte packet. Hence, the basic coverage of all the systems is extended consequently. Besides, the smaller packet is less sensitive to the higher MCS and higher Doppler effect and thus can fulfill a more rigorous PRR requirement. Faced with the most challenging environment, the highway NLOS scenario, there is still $109\ \mathrm{m}$ available in the basic coverage for MCS 5 with the 90% PRR target. Hence, the smaller packet is more favorable and more robust in the ultra-reliable communication where the large transmission coverage can be guaranteed.

In lieu of the monotonic increase with the decreasing distance, the casual reduction of the PRR emerges for MCS 5 in the 1×2 and 2×2 systems under both scenarios and for MCS 1 in the 2×1 and 2×2 systems under the highway NLOS scenario.

In addition, the higher distance threshold for the PRR with the smaller packet shortens the long-distance range over which the advantageous multi-antenna configurations are activated.

4.2.2.2.2 1500-byte packet. As the result of the reduced PRR and coverage, the basic coverage is narrowed and even cannot be realized in the highway NLOS scenario for MCS 5 since the 1500-byte packet is more vulnerable to the higher MCS and higher Doppler effect.

In comparison with the 100-byte packet, the abnormal decrease of the PRR appears excluding the 2×2 system for MCS 5 in the urban NLOS scenario and including the 2×1 system for MCS 5 in the highway NLOS scenario.

4.2.2.3 Impact of MCS.

4.2.2.3.1 MCS 1. With the higher PRR and the larger coverage usually achieved by MCS 1, the basic coverage is accordingly enlarged in contrast with MCS 5. More resistant to the larger packet size and higher Doppler effect, the basic coverage of $283\ \text{m}$ can still be guaranteed even in the highway NLOS scenario with the 1500-byte packet. Thus, the lower MCS is superior in the reliability and robustness of the communication with the extension of the transmission coverage.

Other than the monotonic rise with the decrease of the distance in the long-distance range, the undesired drop of the PRR in the short-distance range happens in the 2×1 and 2×2 systems with both packet sizes under the highway NLOS scenario.

Additionally, the distance threshold of the PRR for MCS 1 is greatly increased and hence the long-distance range which motivates the beneficial multi-antenna system is extremely reduced.

4.2.2.3.2 MCS 5. The PRR and coverage of MCS 5 descend more significantly, especially for the larger packet size and higher Doppler effect. More seriously, the basic coverage in the highway NLOS scenario with the 1500-byte packet is disabled.

The accidental decline of the PRR exists in the 1×2 and 2×2 systems with the 100-byte packet for both scenarios, in the 1×2, 2×1, and 2×2 systems with the 1500-byte packet for the highway NLOS scenario, and in the 1×2 system with the 1500-byte packet for the urban NLOS scenario.

4.2.2.4 Impact of V2V scenario.

4.2.2.4.1 Urban NLOS scenario. Generally, the PRR undergoes the monotonic growth with the reduction of the distance and enters the stability subsequently in the urban scenario with a lower Doppler effect. However, there is an unusual decline of the PRR for MCS 5 in the 1×2 and 2×2 systems with the 100-byte packet and in the 1×2 system with the 1500-byte packet in agreement with the undesired rise of the PER.

Less affected by the larger packet size and higher MCS, the transmission coverage is less limited accompanied by the higher PRR. The basic coverage is always larger compared with the highway NLOS scenario due to the common extension on the coverage of each antenna configuration. Moreover, the basic coverage is still valid for $49\ \text{m}$ even with the 1500-byte packet for MCS 5.

The distance threshold above which the PRR of various antenna configurations can be distinguished is larger than or equal to that in the highway NLOS scenario for MCS 1 and MCS 5 and hence generates a smaller or equal long-distance range within which the multi-antenna configurations are helpful.

4.2.2.4.2 Highway NLOS scenario. The PRR, as well as the transmission coverage, is usually a bit smaller in the highway scenario than that in the urban scenario arising from the higher Doppler effect.

The unexpected drop of the PRR occurs with both packet sizes for MCS 1 in the

2×1 and 2×2 systems and for MCS 5 in the 1×2 and 2×2 systems, and solely with the 1500-byte packet for MCS 5 in the 2×1 system.

The deterioration of the PRR with the 1500-byte packet for MCS 5 becomes more severe and the coverage is greatly restricted. Accordingly, the PRRs in the 2×1 and 2×2 systems are always below 90% and thus invalidate the basic coverage regarding the 90% PRR requirement.

The impact of all the parameters, including the antenna configuration, packet size, MCS, and V2V scenario, on the PRR for IEEE 802.11bd are concluded in Table 4.16 with the applicable range indicated.

Table 4.16 Impact of parameters on PRR for IEEE 802.11bd

Parameter	PRR
Antenna Configuration	MIMO>SIMO>MISO>SISO (Above distance threshold)
Packet Size	100 bytes>1500 bytes (Mostly)
MCS	MCS 1>MCS 5 (Mostly)
V2V Scenario	Urban NLOS>Highway NLOS (Mostly)

4.2.3 Output Packet IAT

The simulation results of the output packet IAT for IEEE 802.11bd with the 100-

byte and 1500-byte packets are demonstrated under the urban NLOS scenario in Fig. 4.8 (a) and Fig. 4.8 (b) and under the highway NLOS scenario in Fig. 4.8 (c) and Fig. 4.8 (d), respectively. A few areas have been enlarged to display the requisite details which cannot be neglected in the following analysis.

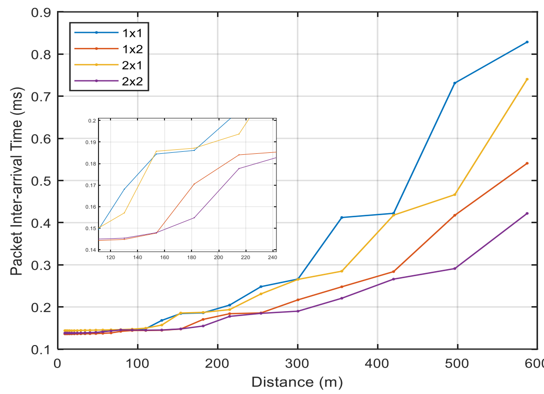

(a) Urban NLOS scenario with the 100-byte packet

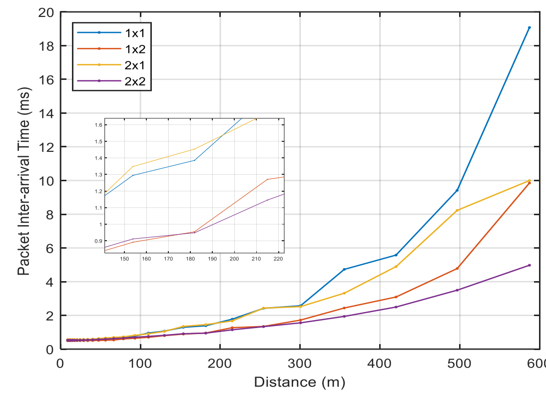

(b) Urban NLOS scenario with the 1500-byte packet

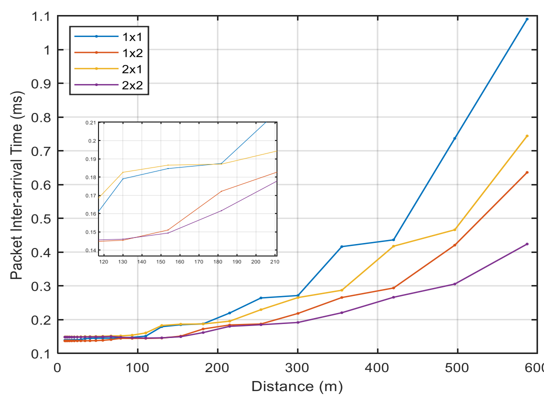

(c) Highway NLOS scenario with the 100-byte packet

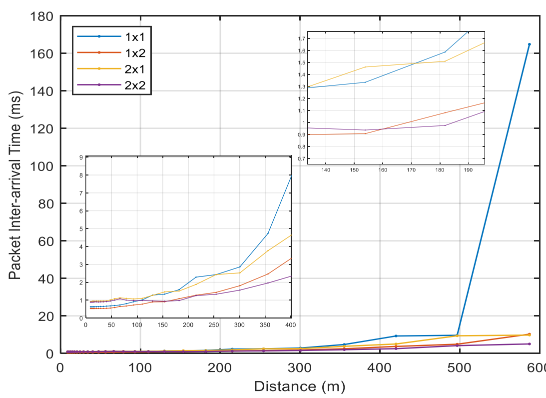

(d) Highway NLOS scenario with the 1500-byte packet

Figure 4.8 Output packet IAT in urban NLOS and highway NLOS scenarios with the 100-byte and 1500-byte packets for IEEE 802.11bd

4.2.3.1 Impact of antenna configuration.

4.2.3.1.1 SISO. The output packet IAT of the SISO (1×1) system, which always monotonically descends with the decline of the distance for both packet sizes in both scenarios, keeps largest above the distance threshold.

Most sensitive to the larger packet size and higher Doppler effect, the packet IAT is dramatically increasing with the growth of the distance in the highway NLOS scenario with the 1500-byte packet and the resulting packet IAT at the farthest distance is as high as $165\ \text{ms}$.

4.2.3.1.2 MISO. The output packet IAT of the MISO (2×1) system is reduced in contrast with the SISO system beyond the distance threshold. The abnormal growth of the packet IAT only occurs in the highway NLOS scenario with the 1500-byte packet and is located between $93\ \text{m}$ and $67\ \text{m}$, otherwise, the packet IAT maintains the monotonic reduction with the decrease of the distance.

4.2.3.1.3 SIMO. Based on the monotonic drop with the decline of the distance under both scenarios with both packet sizes, the output packet IAT of the SIMO (1×2) system can be further decreased compared with the MISO and SISO systems above the distance threshold.

4.2.3.1.4 MIMO. With the smallest output packet IAT beyond the distance threshold, the MIMO (2×2) system surpasses all the other systems. On one hand, the monotonic reduction of the packet IAT with the decreasing distance exclusively appears in the urban NLOS scenario with the 1500-byte packet. On the other hand, the unusual raise of the packet IAT extensively happens in all the other three instances where it is situated between $110\ \text{m}$ and $79\ \text{m}$ under the urban NLOS scenario with the 100-byte packet, between $110\ \mathrm{m}$ and $67\ \mathrm{m}$ under the highway NLOS scenario with the 100-byte packet, and between $154\ \mathrm{m}$ and $67\ \mathrm{m}$ under the highway NLOS scenario with the 1500-byte packet, respectively.

Regardless of the multi-antenna interference within the short distance which sometimes gives rise to the larger packet IAT of the multi-antenna systems in contrast with the SISO system, the multi-antenna configurations are still beneficial in utilizing the multipath components at the longer distance where the multi-antenna systems are superior to the SISO system with the smaller packet IAT above the threshold. Accordingly, the distance thresholds of the output packet IAT respectively with the 100-byte and 1500-byte packets under the urban NLOS and highway NLOS scenarios are listed in Table 4.17.

Table 4.17 Distance thresholds (m) for output packet IAT with IEEE 802.11bd

V2V Scenario	100 bytes	1500 bytes
Urban NLOS	185	195
Highway NLOS	177	171

4.2.3.2 Impact of packet size.

4.2.3.2.1 100-byte packet. Always with the smaller output packet IAT which is favorable in the low-latency application, the reduction with the descending distance is gentle and the undesired increase exists in the 2×2 system for both scenarios. More robust to the higher Doppler effect, the deterioration of the packet IAT in the highway NLOS scenario is greatly alleviated.

The smaller distance threshold in the urban NLOS scenario and the larger distance threshold in the highway NLOS scenario compared to the 1500-byte packet are obtained according to the adaptation on all the MCSs.

4.2.3.2.2 1500-byte packet. During the sharp growth of the packet IAT with the ascending distance, the resulting packet IAT is increased significantly compared to that with the 100-byte packet and the deviation between both scenarios becomes more prominent with the larger packet size. The abnormal growth of the packet IAT with the decreasing distance appears in the 2×1 and 2×2 systems under the highway NLOS scenario.

4.2.3.3 Impact of V2V scenario.

4.2.3.3.1 Urban NLOS scenario. The output packet IAT is generally smaller in the urban NLOS scenario than that in the highway NLOS scenario, and the gap increases for the larger packet size. Consequently, the urban NLOS scenario is more tolerant than the highway NLOS scenario which becomes more evident for the larger packet size.

Besides, the larger distance threshold above which the packet IAT of all the systems can be isolated confines the long-distance range where the advantage of the multi-antenna configurations can be initiated.

4.2.3.3.2 Highway NLOS scenario. The growth of the packet IAT compared to the urban NLOS scenario is slight with the 100-byte packet but becomes more conspicuous with the 1500-byte packet, especially at the farthest distance in the 1×1 system which results in an incomparable packet IAT.

In addition to the 2×2 system with the 100-byte packet under the urban NLOS scenario, the abnormal rise of the packet IAT with the decline of the distance occurs more widely in the highway NLOS scenario including the 2×2 system with the 100-byte packet and the 2×1 and 2×2 systems with the 1500-byte packet.

The impact of all the parameters, including the antenna configuration, packet size, and V2V scenario, on the output packet IAT for IEEE 802.11bd are concluded in Table 4.18 with the applicable range indicated.

Table 4.18 Impact of parameters on output packet IAT for IEEE 802.11bd

Parameter	Output Packet IAT
Antenna Configuration	MIMO<SIMO<MISO<SISO (Above distance threshold)
Packet Size	100 bytes<1500 bytes (Always)
V2V Scenario	Urban NLOS<Highway NLOS (Mostly)

4.2.4 Output Effective Data Rate

The simulation results of the output effective data rate for IEEE 802.11bd with the 100-byte and 1500-byte packets are displayed under the urban NLOS scenario in Fig. 4.9 (a) and Fig. 4.9 (b) and under the highway NLOS scenario in Fig. 4.9 (c) and Fig. 4.9 (d), respectively.

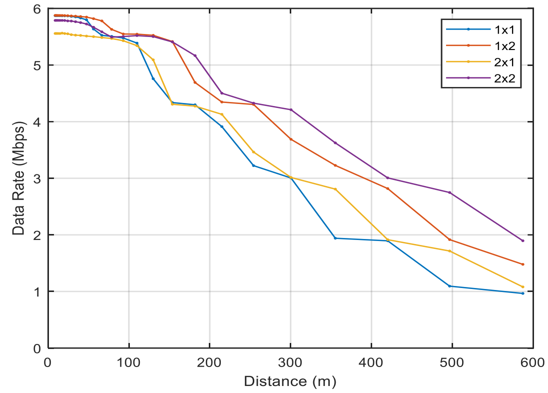

(a) Urban NLOS scenario with the 100-byte packet

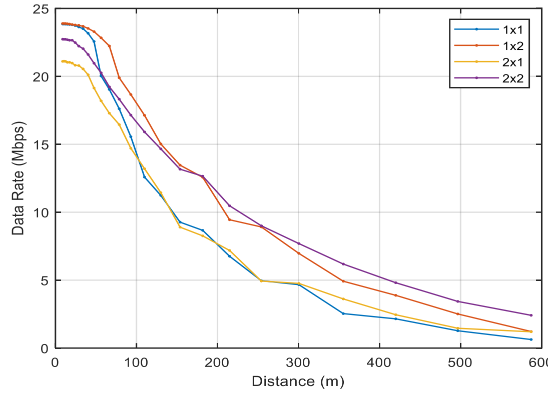

(b) Urban NLOS scenario with the 1500-byte packet

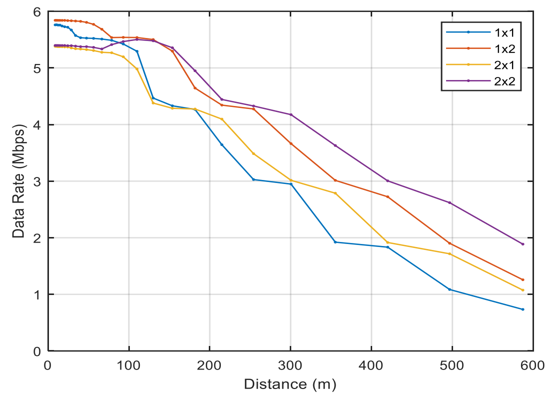

(c) Highway NLOS scenario with the 100-byte packet

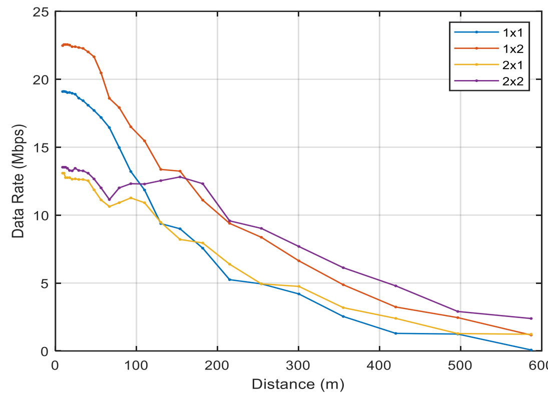

(d) Highway NLOS scenario with the 1500-byte packet

Figure 4.9 Output effective data rate in urban NLOS and highway NLOS scenarios with the 100-byte and 1500-byte packets for IEEE 802.11bd

4.2.4.1 Impact of antenna configuration.

4.2.4.1.1 SISO. The output effective data rate of the SISO (1×1) system always experiences the monotonic increase with the descending distance for both scenarios and both packet sizes and remains lowest among all the antenna configurations beyond a specific distance threshold.

4.2.4.1.2 MISO. The output effective data rate of the MISO (2×1) system is enhanced compared to the SISO system above the distance threshold. Except for the highway NLOS scenario with the 1500-byte packet where there is an obvious decline ranging from 93 m to 67 m, the data rate keeps monotonically increasing with the decreasing distance.

4.2.4.1.3 SIMO. The output effective data rate of the SIMO (1×2) system undergoes monotonic growth with the reducing distance including both scenarios and both packet sizes and can be further elevated compared to the MISO as well as the SISO systems beyond the distance threshold.

4.2.4.1.4 MIMO. The MIMO (2×2) system outperforms all the other systems with the highest output effective data rate above the distance threshold. Instead of the monotonic increase with the decline of the distance which only occurs in the urban NLOS scenario with the 1500-byte packet, an evident reduction in the data rate exists in all the other three situations. Specifically, it is located from 110 m to 79 m in the urban NLOS scenario with the 100-byte packet, from 110 m to 67 m in the highway NLOS scenario with the 100-byte packet, and from 154 m to 67 m in the highway NLOS scenario with the 1500-byte packet, respectively.

Different from the interference which is generated by the multi-antenna systems in the short distance and leads to the lower data rate of some multi-antenna systems compared with the SISO system, the multipath components can be exploited by the multi-antenna configurations at the farther distance defined by the threshold above which the data rate of the multi-antenna systems are higher than that in the SISO system. Specifically, the distance thresholds of the output effective data rate respectively with the 100-byte and 1500-byte packets in the urban NLOS and highway NLOS scenarios are shown in Table 4.19.

Table 4.19 Distance thresholds (m) for output effective data rate with IEEE 802.11bd

V2V Scenario	100 bytes	1500 bytes
Urban NLOS	185	198
Highway NLOS	177	173

4.2.4.2 Impact of packet size.

4.2.4.2.1 100-byte packet. The output effective data rate is lower with the 100-byte packet and generally undergoes a gradual increase with the reduction in distance. The unpopular drop is present in the 2×2 system under both the urban NLOS and highway NLOS scenarios. Less vulnerable to the higher Doppler effect, the difference between the urban and highway scenarios are notably suppressed.

The distance threshold is smaller in the urban NLOS scenario and larger in the highway NLOS scenario compared to the 1500-byte packet, as the result of the optimal selection on all the MCSs.

4.2.4.2.2 1500-byte packet. After the steep decrease with the increase of the distance, the minimum data rate at the farthest distance becomes comparable to that with the 100-byte packet. However, the higher data rate over most of the distance range is still more beneficial for the high-throughput application.

The significant deterioration of the data rate is generated with the higher Doppler effect especially at the short distance within 200 m, and the temporary reduction with the decline of the distance emerges in the 2×1 and 2×2 systems under the highway NLOS scenario.

4.2.4.3 Impact of V2V scenario.

4.2.4.3.1 Urban NLOS scenario. The output effective data rate under the urban NLOS scenario is usually higher compared to the highway NLOS scenario, and the difference becomes more remarkable with the larger packet size. Hence, the urban NLOS scenario is less stringent than the highway NLOS scenario which becomes more obvious for the challenging larger packet.

Moreover, the larger distance threshold beyond which the data rate of various systems can be separated implies a smaller long-distance range where the multi-antenna configurations are advantageous.

4.2.4.3.2 Highway NLOS scenario. The exacerbation of the data rate compared with the urban NLOS scenario becomes even worse with the larger packet size. Specifically, the initial data rates of all the systems at the shortest distance in the urban NLOS scenario with the 1500-byte packet can remain higher than $20\ \text{Mbps}$, but in the highway NLOS scenario with the 1500-byte packet, except for the 1×2 system, the initial data rates of all the other three systems fall below $20\ \text{Mbps}$.

Different from the urban NLOS scenario where the undesired sink of the data rate during the decrease of the distance only exists in the 2×2 system with the 100-byte packet, the casual drop appears not only in the 2×2 system with the 100-byte packet but also in the 2×1 and 2×2 systems with the 1500-byte packet under the highway NLOS scenario.

The impact of all the parameters, including the antenna configuration, packet size, and V2V scenario, on the output effective data rate for IEEE 802.11bd are concluded in Table 4.20 with the applicable range indicated.

Table 4.20 Impact of parameters on output effective data rate for IEEE 802.11bd

Parameter	Output Effective Data Rate
Antenna Configuration	MIMO>SIMO>MISO>SISO (Above distance threshold)
Packet Size	1500 bytes>100 bytes (Mostly)
V2V Scenario	Urban NLOS>Highway NLOS (Mostly)

CHAPTER FIVE

CONCLUSION

In this proposed work, the complete PHY performance of both IEEE 802.11p and IEEE 802.11bd are sufficiently investigated and evaluated in terms of the PER, PRR, output packet IAT, and output effective data rate. Various antenna, packet, and MCS configurations are studied under both the urban NLOS and highway NLOS scenarios to explore the impact of the antenna configuration, packet size, MCS, and Doppler effect on the PHY performance. Some specific conclusions are summarized as follows.

- The MIMO system performs best with the lowest PER, largest PRR and transmission coverage, smallest output packet IAT, and highest output effective data rate, at the distance above the distance threshold which corresponds to the SNR below the SNR threshold [57]. On the contrary, the SISO system is the least beneficial with the worst performance and is most vulnerable to the larger packet, higher MCS, and higher Doppler effect. The performance of the SIMO and MISO systems is in between that of the MIMO and SISO systems, and the SIMO system is better than the MISO system although there are equal multiple antennas at the transmitter in the MISO system and at the receiver in the SIMO system.
- The smaller packet, which is less sensitive to the higher MCS and higher Doppler effect, is more favorable for the high-reliability and low-latency communications based on its lower PER, larger PRR and transmission coverage, and smaller output packet IAT. Meanwhile, the larger packet that can achieve a higher output effective data rate is more beneficial in the high-throughput communications.

- The lower MCS, that is less susceptible to the larger packet and higher Doppler effect, is more conducive in the high-reliability communications due to its lower PER, higher PRR, and larger transmission coverage. On the other hand, the higher MCS can realize the smaller output packet IAT for the low-latency communications and the higher output effective data rate for the high-throughput communications.
- Depending on the slight superiority in reducing the PER, increasing the PRR and transmission coverage, decreasing the output packet IAT, and enhancing the output effective data rate compared to the highway NLOS scenario with the higher Doppler effect, the urban NLOS scenario with the lower Doppler effect is more resistant to the larger packet and higher MCS.

REFERENCES

[1] G. Naik, B. Choudhury, and J.-M. Park, "IEEE 802.11bd & 5G NR V2X: Evolution of radio access technologies for V2X communications," *IEEE Access*, vol. 7, pp. 70169–70184, 2019.

[2] K. Kiela, V. Barzdenas, M. Jurgo, V. Macaitis, J. Rafanavicius, A. Vasjanov, L. Kladovscikov, and R. Navickas, "Review of V2X–IoT standards and frameworks for ITS applications," *Applied Sciences*, vol. 10, no. 12, p. 4314, Jun. 2020.

[3] F. Arena, G. Pau, and A. Severino, "A review on IEEE 802.11p for intelligent transportation systems," *Journal of Sensor and Actuator Networks*, vol. 9, no. 2, p. 22, Apr. 2020.

[4] X. Huang, D. Zhao, and H. Peng, "Empirical study of DSRC performance based on safety pilot model deployment data," *IEEE Transactions on Intelligent Transportation Systems*, vol. 18, no. 10, pp. 2619–2628, Oct. 2017.

[5] L. Cheng, B. E. Henty, D. D. Stancil, F. Bai, and P. Mudalige, "Mobile vehicle-to-vehicle narrow-band channel measurement and characterization of the 5.9 GHz dedicated short range communication (DSRC) frequency band," *IEEE Journal on Selected Areas in Communications*, vol. 25, no. 8, pp. 1501–1516, Oct. 2007.

[6] W. Anwar, S. Dev, A. Kumar, N. Franchi, and G. Fettweis, "PHY abstraction techniques for V2X enabling technologies: modeling and analysis," *IEEE Transactions on Vehicular Technology*, vol. 70, no. 2, pp. 1501–1517, Feb. 2021.

[7] J. Choi, V. Marojevic, C. B. Dietrich, J. H. Reed, and S. Ahn, “Survey of spectrum regulation for intelligent transportation systems,” *IEEE Access*, vol. 8, pp. 140145–140160, 2020.

[8] K. Ansari, “Joint use of DSRC and C-V2X for V2X communications in the 5.9 GHz ITS band,” *IET Intelligent Transport Systems*, vol. 15, no. 2, pp. 213–224, Feb. 2021.

[9] *IEEE Standard for Information Technology-Telecommunications and Information Exchange between Systems Local and Metropolitan Area Networks-Specific Requirements—Part 11: Wireless LAN Medium Access Control (MAC) and Physical Layer (PHY) Specifications*, Standard 802.11-2020 (Revision of IEEE Std 802. 11–2016), 2020.

[10] R. Cao, H. Zhang, and P. Sharma, *Potential PHY Designs for NGV*, Standard 802.11-19/0016r0, Jan. 2019.

[11] B. Sadeghi, *802.11bd Specification Framework Document*, Standard 802.11-15/0132r07, Sep. 2019.

[12] V. Torgunakov, V. Loginov, and E. Khorov, “A Study of Channel Bonding in IEEE 802.11bd Networks,” *IEEE Access*, vol. 10, pp. 25514–25533, 2022.

[13] W. Anwar, N. Franchi, and G. Fettweis, “A study on link adaptation techniques for IEEE 802.11bd based eV2X communications,” in *2021 IEEE 94th Vehicular Technology Conference (VTC2021-Fall)*, Sep. 2021, pp. 1–7.

[14] *IEEE Standard for Information Technology-Telecommunications and Information Exchange between Systems Local and Metropolitan Area Networks-Specific Requirements—Part 11: Wireless LAN Medium Access Control (MAC) and Physical*

Layer (PHY) Specifications Amendment 5: Enhancements for Next Generation V2X, IEEE Standard 802.11bd, 2022.

[15] *TSG SA, Release Description; Release 14*, document TR 21.914 V14.0.0, 3GPP, Jun. 2018.

[16] D. Garcia-Roger, E. E. González, D. Martín-Sacristán, and J. F. Monserrat, “V2X support in 3GPP specifications: From 4G to 5G and beyond,” *IEEE Access*, vol. 8, pp. 190946–190963, 2020.

[17] *TSG SA, Release Description; Release 16*, document TR 21.916 V16.2.0, 3GPP, Jun. 2022.

[18] N. Patriciello, S. Lagen, B. Bojovic, and L. Giupponi, “An E2E simulator for 5G NR networks,” *Simulation Modelling Practice and Theory*, vol. 96, Nov. 2019, Art. no. 101933.

[19] 5G Automotive Association. (Dec. 2017). *An Assessment of LTE-V2X (PC5) and 802.11p Direct Communications Technologies for Improved Road Safety in the EU*. [Online]. Available: https://5gaa.org/wp-content/uploads/2017/12/5GAA-Road-safety-FINAL2017-12-05.pdf

[20] 5G Automotive Association. (Oct. 2018). *V2X Functional and Performance Test Report; Test Procedures and Results*. 5GAA P-190033. [Online]. Available: https://5gaa.org/wp-content/uploads/2018/11/5GAA_P-190033_V2X-Functional-and-Performance-Test-Report_final-1.pdf

[21] 5G Automotive Association. (Oct. 2018). *V2X Technology Functional and Performance Benchmark Testing Key Findings*. [Online]. Available:

https://5gaa.org/wp-content/uploads/2018/10/FCC-USDOT-CV2X-v2.14_wo_Video-c1_Final.pdf

[22] A. Bazzi, G. Cecchini, M. Menarini, B. M. Masini, and A. Zanella, “Survey and perspectives of vehicular Wi-Fi versus sidelink cellular-V2X in the 5G era,” *Future Internet*, vol. 11, no. 6, p. 122, May 2019.

[23] Z. Hameed Mir and F. Filali, “LTE and IEEE 802.11p for vehicular networking: a performance evaluation,” *EURASIP Journal on Wireless Communications and Networking*, vol. 2014, no. 1, p. 89, May 2014.

[24] A. Bazzi, B. M. Masini, A. Zanella, and I. Thibault, “On the performance of IEEE 802.11p and LTE-V2V for the cooperative awareness of connected vehicles,” *IEEE Transactions on Vehicular Technology*, vol. 66, no. 11, pp. 10419–10432, Nov. 2017.

[25] *IEEE Guide for Wireless Access in Vehicular Environments (WAVE) Architecture*, Standard 1609.0-2019, 2019.

[26] A. Triwinarko, I. Dayoub, and S. Cherkaoui, “PHY layer enhancements for next generation V2X communication,” *Vehicular Communications*, vol. 32, Dec. 2021, Art. no. 100385.

[27] B. Y. Yacheur, T. Ahmed, and M. Mosbah, “Analysis and comparison of IEEE 802.11p and IEEE 802.11bd,” in *Communication Technologies for Vehicles*, F. Krief, H. Aniss, L. Mendiboure, S. Chaumette, and M. Berbineau, Eds. Cham, Switzerland: Springer, 2020, pp. 55–65.

[28] X. Ma and K. S. Trivedi, "SINR-based analysis of IEEE 802.11p/bd broadcast VANETs for safety services," *IEEE Transactions on Network and Service Management*, vol. 18, no. 3, pp. 2672–2686, Sep. 2021.

[29] T. Petrov, P. Pocta, and T. Kovacikova, "Benchmarking 4G and 5G-based cellular-V2X for vehicle-to-infrastructure communication and urban scenarios in cooperative intelligent transportation systems," *Applied Sciences*, vol. 12, no. 19, p. 9677, Sep. 2022.

[30] R. Liu, D. N. Aloi, "A rigorous analysis of vehicle-to-vehicle range performance in a rural channel propagation scenario as a function of antenna type and location via simulation and field trails," *China Communications*, vol. 20, no. 11, pp. 131–141, 2023.

[31] W. Anwar, N. Franchi, and G. Fettweis, "Physical layer evaluation of V2X communications technologies: 5G NR-V2X, LTE-V2X, IEEE 802.11bd, and IEEE 802.11p," in *2019 IEEE 90th Vehicular Technology Conference (VTC2019-Fall)*, Sep. 2019, pp. 1–7.

[32] T. Petrov, L. Sevcik, P. Pocta, and M. Dado, "A performance benchmark for dedicated short-range communications and LTE-based cellular-V2X in the context of vehicle-to-infrastructure communication and urban scenarios," *Sensors*, vol. 21, no. 15, p. 5095, Jul. 2021.

[33] J. Zhao, X. Gai, and X. Luo, "Performance comparison of vehicle networking based on DSRC and LTE technology," in *2021 6th International Conference on Intelligent Transportation Engineering (ICITE 2021)*, Z. Zhang, Ed. Singapore: Springer, 2022, pp. 730–746.

[34] V. Maglogiannis, D. Naudts, S. Hadiwardoyo, D. van den Akker, J. Marquez-Barja, and I. Moerman, "Experimental V2X evaluation for C-V2X and ITS-G5 technologies in a real-life highway environment," *IEEE Transactions on Network and Service Management*, vol. 19, no. 2, pp. 1521–1538, Jun. 2022.

[35] M. Karoui, A. Freitas, and G. Chalhoub, "Performance comparison between LTE-V2X and ITS-G5 under realistic urban scenarios," in *2020 IEEE 91st Vehicular Technology Conference (VTC2020-Spring)*, May 2020, pp. 1–7.

[36] R. Jacob, W. Anwar, N. Schwarzenberg, N. Franchi, and G. Fettweis, "System-level performance comparison of IEEE 802.11p and 802.11bd draft in highway scenarios," in *2020 27th International Conference on Telecommunications (ICT)*, Oct. 2020, pp. 1–6.

[37] W. Anwar, A. Traßl, N. Franchi, and G. Fettweis, "On the reliability of NR-V2X and IEEE 802.11bd," in *2019 IEEE 30th Annual International Symposium on Personal, Indoor and Mobile Radio Communincations (PIMRC)*, Sep. 2019, pp. 1–7.

[38] S. Zeadally, M. A. Javed, and E. B. Hamida, "Vehicular communications for ITS: Standardization and challenges," *IEEE Communications Standards Magazine*, vol. 4, no. 1, pp. 11–17, Mar. 2020.

[39] J. B. Kenney, "Dedicated short-range communications (DSRC) standards in the United States." *Proceedings of the IEEE*, vol. 99, no. 7, pp.1162–1182, Jul. 2011.

[40] U. K. Dey, R. Akl, R. Chataut, and M. Robaei, "Selective MIMO in vehicular communication for reliable safety services and high speed non-safety services," in *2021 IEEE 12th Annual Ubiquitous Computing, Electronics & Mobile Communication Conference (UEMCON)*, Dec. 2021, pp. 0785–0790.

[41] D. Shukla, V. Kumar, and A. Prakash, “Performance evaluation of IEEE 802.11p physical layer for efficient vehicular communication,” in *Advances in VLSI, Communication, and Signal Processing*, D. Dutta, H. Kar, C. Kumar, and V. Bhadauria Eds. Singapore: Springer, 2020, pp. 51–60.

[42] B. Sun and H. Zhang, *802.11 NGV Proposed PAR*, Standard 802.11-18/0861r9, Nov. 2018.

[43] A. Grami, *Introduction to Digital Communications*. Oxford, U.K.: Academic Press, 2016, pp. 493–511.

[44] T. Suzuki, and Y. Amano, “NLOS multipath classification of GNSS signal correlation output using machine learning,” *Sensors*, vol. 21, no. 7, p. 2503, Apr. 2021.

[45] V. K. Garg, *Wireless Communications and Networking*. San Francisco, CA, USA: Morgan Kaufmann Publishers, 2007, pp. 47–84.

[46] S. Guo, D. N. Aloi, J. Li, and H. Zhao, “MIMO-based physical layer evaluation on IEEE 802.11bd,” *IEEE Access*, vol. 11, pp. 115511–115528, 2023.

[47] E. Biglieri, R. Calderbank, A. Constantinides, A. Goldsmith, A. Paulraj, and H. V. Poor, *MIMO Wireless Communications*. Cambridge, U.K.: Cambridge University Press, 2007, pp. 1–19.

[48] F. De Flaviis, L. Jofre, J. Romeu, and A. Grau, *Multi-Antenna Systems for MIMO Communications*. San Rafael, CA, USA: Morgan & Claypool, 2008, pp. 1–65.

[49] M. Kahn, *V2V Radio Channel Models*, Standard 802.11-14/0259r0, Feb. 2014.

[50] J. R. Hampton, *Introduction to MIMO Communications*. Cambridge, U.K.: Cambridge University Press, 2014, pp. 1–69.

[51] A. Bensky, *Short-Range Wireless Communication*, 3rd ed. Oxford, U.K.: Newnes, 2019, pp. 11–41.

[52] B. Sklar and F. J. Harris, *Digital Communications: Fundamentals and Applications*, 3rd ed. Hoboken, NJ, USA: Pearson, 2021, pp. 971–1088.

[53] T.-D. Chiueh, P.-Y. Tsai, and I.-W. Lai, *Baseband Receiver Design for Wireless MIMO-OFDM Communications*. 2nd ed. Singapore: Wiley, 2012, pp. 39–53.

[54] A. Zaidi, F. Athley, J. Medbo, U. Gustavsson, G. Durisi, and X. Chen, *5G Physical Layer: Principles, Models and Technology Components*. Oxford, U.K.: Academic Press, 2018, pp. 119–125.

[55] B. Ahmed and M. A. Matin, *Coding for MIMO-OFDM in Future Wireless Systems*. New York, NY, USA: Springer, 2015, pp. 1–26.

[56] J. Yin, T. ElBatt, G. Yeung, B. Ryu, S. Habermas, H. Krishnan, and T. Talty, "Performance evaluation of safety applications over DSRC vehicular ad hoc networks," in *Proceedings of the 1st ACM international workshop on Vehicular ad hoc networks*, Oct. 2004, pp. 1–9.

[57] L. Hanzo, Y. Akhtman, L. Wang, and M. Jiang, *MIMO-OFDM for LTE, Wi-Fi and WiMAX: Coherent versus Non-coherent and Cooperative Turbo-transceivers*. Chichester, U. K.: Wiley, 2011, pp. 1–36.

[58] T. Hwang, C. Yang, G. Wu, S. Li, and G. Y. Li, "OFDM and its wireless applications: A survey," *IEEE Transactions on Vehicular Technology*, vol. 58, no. 4, pp. 1673–1694, May 2009.

[59] H. Asplund, D. Astely, P. von Butovitsch, T. Chapman, M. Frenne, F. Ghasemzadeh, M. Hagström, B. Hogan, G. Jöngren, J. Karlsson, F. Kronestedt, and E. Larsson, *Advanced Antenna Systems for 5G Network Deployments: Bridging the Gap between Theory and Practice*. Oxford, U.K.: Academic Press, 2020, pp. 133–159.

[60] A. Paulraj, R. Nabar, and D. Gore, *Introduction to Space-Time Wireless Communications*. Cambridge, U.K.: Cambridge University Press, 2003, pp. 178–198.

[61] T. J. Rouphael, *RF and Digital Signal Processing for Software-defined Radio: A Multi-Standard Multi-Mode Approach*. Oxford, U.K.: Newnes, 2009, pp. 65–71.

[62] S. Chen and A. M. Wyglinski, "Digital communication fundamentals for cognitive radio," in *Cognitive Radio Communications and Networks: Principles and Practice*, A. M. Wyglinski, M. Nekovee, and T. Hou, Eds. Oxford, U.K.: Academic Press, 2010, pp. 57–72.

[63] S. K. Wilson, O. A. Dobre, "Multicarrier transmission in a frequency-selective channel," in *Academic Press Library in Mobile and Wireless Communications: Transmission Techniques for Digital Communications*, S. K. Wilson, S. Wilson, and E. Biglieri, Eds. Oxford, U.K.: Academic Press, 2016, pp. 333–367.

[64] C. F. Mecklenbrauker, A. F. Molisch, J. Karedal, F. Tufvesson, A. Paier, L. Bernadó, T. Zemen, O. Klemp, and N. Czink, "Vehicular channel characterization and its implications for wireless system design and performance," *Proceedings of the IEEE*, vol. 99, no. 7, pp.1189–1212, Jul. 2011.

[65] R. W. Heath, Jr. and A. Lozano, *Foundations of MIMO Communication*. Cambridge, U.K.: Cambridge University Press, 2019, pp. 77–110.

[66] Z. Rafique, and B.-C. Seet, “Energy-efficient MIMO–OFDM systems,” in *Handbook of Green Information and Communication Systems*, M. S. Obaidat, A. Anpalagan, and I. Woungang, Eds. Oxford, U.K.: Academic Press, 2013, pp. 393–422.

[67] A. El-Keyi, T. ElBatt, F. Bai, and C. Saraydar, “MIMO VANETs: Research challenges and opportunities,” in *2012 International Conference on Computing, Networking and Communications (ICNC)*, Jan. 2012, pp. 670–676.

[68] K. Raoof, M. B. Zid, N. Prayongpun, and A. Bouallegue, “Advanced MIMO techniques: Polarization diversity and antenna selection” in *MIMO Systems, Theory and Applications*, H. K. Bizaki, Ed. Norderstedt, Germany: BoD–Books on Demand, 2011, pp. 3–56.

[69] L. Cazzella, D. Tagliaferri, M. Mizmizi, D. Badini, C. Mazzucco, M. Matteucci, and U. Spagnolini, “Deep learning of transferable MIMO channel modes for 6G V2X communications,” *IEEE Transactions on Antennas and Propagation*, vol. 70, no. 6, pp. 4127–4139, Jun. 2022.

[70] D. J. Love and R. W. Heath, Jr., “Feedback techniques for MIMO channels,” in *MIMO System Technology for Wireless Communications*, G. Tsoulos, Ed. Boca Raton, FL, USA: CRC Press, 2006, pp. 113–146.

[71] H. Huang, C. B. Papadias, and S. Venkatesan, *MIMO Communication for Cellular Networks*. New York, NY, USA: Springer, 2012, pp. 1–19.

[72] B. Clerckx and C. Oestges, *MIMO Wireless Networks: Channels, Techniques and Standards for Multi-Antenna, Multi-User and Multi-Cell Systems*. 2nd ed. Oxford, U.K.: Academic, 2013, pp. 1–27.

[73] S. Nijhawan, A. Gupta, K. Appaiah, R. Vaze, and N. Karamchandani, "Flag manifold-based precoder interpolation techniques for MIMO-OFDM systems," *IEEE Transactions on Communications*, vol. 69, no. 7, pp. 4347–4359, Jul. 2021.

[74] N. Hassan, D. A. Dupleich, C. Schneider, R. Thomä, and G. Del Galdo, "MIMO-TDL model parameter estimation from V2I channel Sounding," in *2021 15th European Conference on Antennas and Propagation (EuCAP)*, Mar. 2021, pp. 1–5.

[75] R. S. Kshetrimayum, *Fundamentals of MIMO Wireless Communications*. Cambridge, U.K.: Cambridge University Press, 2017, pp. 1–11.

[76] B. Kumbhani and R. S. Kshetrimayum, *MIMO Wireless Communications over Generalized Fading Channels*. Boca Raton, FL, USA: CRC Press, 2017, pp. 1–70.

[77] S. Bartoletti, W. Zhuofei, V. Martinez, and A. Bazzi, "A physical layer model for the performance evaluation of V2X communication," *Journal of Latex Class Files*, vol. 14, no. 8, pp. 1–5, Aug. 2021.

[78] I. Sarris (2020) u-blox/ubx-v2x [Source Code]. https://github.com/u-blox/ubx-v2x.

[79] W. Anwar (2020) PHY_abstraction_V2X_technologies-IEEE-802.11p-IEEE802.11bd-LTE-V2X-NR-V2X- [Source Code]. https://github.com/Waqar-Anwar/PHY_abstraction_V2X_technologies-IEEE-802.11p-IEEE802.11bd-LTE-V2X-NR-V2X-.

[80] A. Triwinarko, I. Dayoub, M. Zwingelstein-Colin, M. Gharbi, and B. Bouraoui, "A PHY/MAC cross-layer design with transmit antenna selection and power adaptation

for receiver blocking problem in dense VANETs," *Vehicular Communications*, vol. 24, Aug. 2020, Art. no. 100233.

[81] A. J. Paulraj, D. A. Gore, R. U. Nabar, and H. Bolcskei, "An overview of MIMO communications—A key to gigabit wireless," *Proceedings of the IEEE*, vol. 92, no. 2, pp. 198–218, Feb. 2004.